Wu, Q.; Zhang, X.; Peirats-Llobet, M.; Belda Palazón, B.; Wang, X.; Cui, S.; Yu, X.... (2016). Ubiquitin Ligases RGLG1 and RGLG5 Regulate Abscisic Acid Signaling by Controlling the Turnover of Phosphatase PP2CA. Plant Cell. 28(9):2178-2196. doi:10.1105/tpc.16.00364.

Arabidopsis Ubiquitin Ligases RGLG1 and RGLG5 Regulate Abscisic Acid Signaling by Controlling the Turnover of PP2CA

Qian Wu[a,1], Xu Zhang[a,1], Marta Peirats-Llobet[b], Borja Belda-Palazon[b], Xiaofeng Wang[a], Shao Cui[a], Xiangchun Yu[a], Pedro L. Rodriguez[b,2], Chengcai An[a,2]

[a] The State Key Laboratory of Protein and Plant Gene research, College of life sciences, Peking University, Beijing, 100871, P. R. China

[b] Instituto de Biología Molecular y Celular de Plantas, Consejo Superior de Investigaciones Cientificas-Universidad Politecnica de Valencia, ES-46022 Valencia, Spain

[1] These authors contributed equally to this work.

[2] Address correspondence to chcaian@pku.edu.cn and prodriguez@ibmcp.upv.es.

Running title: RGLG1 and RGLG5 promote degradation of PP2CA

The authors responsible for distribution of materials integral to the findings presented in this article in accordance with the policy described in the Instructions for Authors (www.plantcell.org) are: Chengcai An (chcaian@pku.edu.cn) and Pedro L. Rodriguez (prodriguez@ibmcp.upv.es).

ABSTRACT

Abscisic acid (ABA) is an essential hormone for plant development and stress response. ABA signaling is suppressed by clade A PP2Cs, which are key repressors of the pathway through inhibition of ABA-activated SnRK2s. Upon ABA perception, the PYR/PYL/RCAR ABA receptors bind to PP2Cs with high affinity and biochemically inhibit their activity. Whereas this mechanism has been extensively studied, how PP2Cs are regulated at the protein level is only starting to be explored. *Arabidopsis* RING DOMAIN LIGASE5 (RGLG5) belongs to a five-member E3 ubiquitin ligase family whose target proteins remain unknown. We report RGLG5, together with RGLG1, releases PP2C blockade of ABA signaling by mediating PP2CA protein degradation. ABA promotes the interaction of PP2CA with both E3 ligases, which mediate ubiquitination of PP2CA and are required for ABA-dependent PP2CA turnover. Down-regulation of *RGLG1* and *RGLG5* stabilizes endogenous PP2CA, diminishes ABA-mediated responses and the reduced response to ABA in germination assays is suppressed in the *rglg1 amiRrglg5 pp2ca-1* triple mutant, supporting a functional link among these loci. Overall, our data indicate RGLG1 and RGLG5 are important modulators of ABA signaling, and further unveil a mechanism for activation of the ABA pathway by controlling PP2C half-life.

INTRODUCTION

The plant hormone abscisic acid (ABA) regulates many key processes in plants, including seed germination and development and various biotic and abiotic stress responses (Cutler et al., 2010; Finkelstein, 2013) . The ABA signaling pathway is initiated by ABA perception through PYRABACTIN RESISTANCE1 (PYR1)/PYR1-LIKE (PYL)/REGULATORY COMPONENTS OF ABA RECEPTORS (RCAR) family of proteins (Ma et al., 2009; Park et al., 2009; Santiago et al., 2009; Nishimura et al., 2010). This is followed by interaction with and inactivation of clade A protein phosphatase type 2Cs (PP2Cs), such as ABA INSENSITIVE 1 (ABI1) and ABI2, HYPERSENSITIVE TO ABA (HAB1) and HAB2, and PROTEIN PHOSPHATASE 2CA/ABA-HYPERSENSITIVE GERMINATION 3 (PP2CA/AHG3), thereby releasing their inhibition on three ABA-activated SNF1-related protein kinases (SnRK2s), i.e. SnRK2.2/D, 2.3/I and 2.6/E/OST1 (Umezawa et al., 2009; Vlad et al., 2009). Then these SnRK2s activate downstream signaling by phosphorylation of numerous players, including ABA-responsive transcription factors (Fujii et al., 2009; Fujii and Zhu, 2009; Nakashima et al., 2009), ion channels (Geiger et al., 2009; Lee et al., 2009) and other mediators/effectors involved in ABA signaling and action (Umezawa et al., 2013; Wang et al., 2013).

To optimize allocation of resources between growth/development and stress response, plants need to control timing and extent of ABA pathway activation. Previous work has indicated that posttranscriptional modifications such as phosphorylation (Kobayashi et al., 2005; Hubbard et al., 2010; Cai et al., 2014) and ubiquitination (Zhang et al., 2005; Liu and Stone, 2010, 2011; Kelley and Estelle, 2012) are important mechanisms to modulate ABA signaling. The “ABA-PYR/PYL/RCARs-PP2Cs-SnRK2s” core ABA pathway involves multiple members with redundant and non-redundant functions (Park et al., 2009; Fujii and Zhu, 2009; Nakashima et al., 2009; Rubio et al., 2009; Antoni et al., 2013; Zhao et al.,

2014), which likely allows different combinations depending on various environmental stimuli, developmental stages or cell types (Santiago et al., 2009; Szostkiewicz et al., 2010; Gonzalez-Guzman et al., 2012; Antoni et al., 2012). Recently, studies that address protein dynamics of core ABA signaling components have been published (Bueso et al., 2014; Irigoyen et al., 2014; Kong et al., 2015; reviewed by Yu et al., 2016). However, a comprehensive understanding of the mechanisms and components that regulate receptor and clade A PP2C protein levels is still lacking as well as their contribution to the modulation of ABA signaling in different time and developmental stages. For instance, transcription of some *PYR/PYL/RCARs* is repressed whereas that of *PP2Cs* is stimulated in response to ABA (Santiago et al., 2009; Szostkiewicz et al., 2010), indicating there exist a negative feedback transcriptional mechanism to modulate ABA signaling by controlling transcript levels of core elements. In the case of ABI1, it has been demonstrated that ABA induces degradation of the PP2C through PUB12/13 E3 ligases but subsequently up-regulates *ABI1* expression and protein levels (Kong et al., 2015). PUB13-mediated ABI1 ubiquitination in presence of PYR1 was strictly dependent on ABA, whereas in presence of monomeric receptors ABA only increased ABI1 ubiquitination level (Kong et al., 2015). Recent work also indicates ABA receptor proteins, e.g. PYR1, PYL4 and PYL8, can be degraded via an ubiquitination-dependent mechanism through single subunit and CUL4-based E3 ligases, although PYL8 can be protected from degradation by ABA (Bueso et al., 2014; Irigoyen et al., 2014).

Arabidopsis has a RING-type E3 ubiquitin ligase family, named RGLG (RING DOMAIN LIGASE), composed of five members, i.e. RGLG1 to 5 (Yin et al., 2007). RGLG1 and RGLG2 have been reported to affect hormone signaling since the *rglg1 rglg2* double mutant shows altered auxin and cytokinin levels (Yin et al., 2007). RGLG2 catalyzes the formation of ubiquitin Lys-63 linked chains in a heteromeric complex with MMZ2 and AtUBC35 (Yin et al., 2007). Recently we have shown RGLG3 and RGLG4 are essential regulators of the jasmonate pathway (Zhang et al.,

2012; Zhang et al., 2015). However, in these studies, the molecular targets of RGLG1-4 were not identified. In this study we have found PP2CA, a key negative regulator of ABA signaling (Sheen et al., 1998; Kuhn et al., 2006; Yoshida et al., 2006; Rubio et al., 2009; Lee et al., 2009; Brandt et al., 2015), is a target of RGLG1 and RGLG5. ABA enhances the interaction of RGLG1 and RGLG5 with PP2CA, ABI2 and HAB2, and mediates in vitro ubiquitination of these PP2Cs. Both loss-of-function and gain-of-function phenotypes of RGLG1 and RGLG5 reveal their role as positive regulators of ABA signaling in different ABA responses. In particular, we show RGLG1 and RGLG5 mediate ubiquitination of PP2CA *in vitro* and *in vivo*, which leads to ABA-dependent turnover of PP2CA. Using PP2CA antibodies we could demonstrate that in cycloheximide (CHX)-treated seedlings ABA induces degradation of endogenous PP2CA. Thus, our work further uncovers a mechanism to control the activation of the ABA pathway by degradation of repressors of ABA signaling.

RESULTS

Identification of PP2CA as interacting partner of ubiquitin ligases RGLG1 and RGLG5

RGLG5 belongs to the RGLG E3 ligase family (Yin et al., 2007). To date, the biological function and targets of RGLG5 remain unknown. We aimed to identify its interacting partners to elucidate RGLG5 function and accordingly, the yeast two-hybrid (Y2H) approach was employed to screen an *Arabidopsis* cDNA library using RGLG5 as bait. As a result, PP2CA, a key repressor of the ABA pathway (Kuhn et al., 2006; Yoshida et al., 2006; Rubio et al., 2009), was identified as interacting partner of RGLG5. To ascertain whether other RGLG family members interact with PP2CA, the five RGLGs were each coexpressed with PP2CA in yeast for Y2H screening. Both growth assays in selective medium (Figure 1A) and β-galactosidase quantitative assays (Figure 1B) revealed PP2CA interacted with both RGLG1 and RGLG5. Expression in yeast cells of PP2CA fused to the GAL4 activation domain (AD) and RGLG1-5 proteins fused to the GAL4 DNA binding domain (BD) was verified by Western blot analysis (Supplemental Figure 1A). Interestingly, other PP2Cs, namely ABI2 and HAB2, also showed interactions with RGLG1 and RGLG5, but not ABI1 and HAB1, indicating a certain selectivity of these E3 ligases to recognize clade A PP2Cs (Figure 2A; Supplemental Figure 1B). To better address the functional importance of these interactions, we focused on PP2CA for in-depth study. To investigate whether endogenous RGLGs form *in vivo* complex with PP2CA, we followed a coIP/mass spectrometry (MS) approach to identify proteins that co-immunoprecipitated with FLAG-tagged PP2CA expressed in *Arabidopsis (35S$_{pro}$:FLAG-PP2CA)*. In protein extracts obtained from two-week-old seedlings after 6 h ABA and 30 h MG132 treatment, but not in mock-treated samples, we found native RGLG1 co-immunoprecipitated with FLAG-PP2CA, suggesting ABA promoted *in vivo* association of PP2CA and RGLG1 (Figure 1C; Supplemental Table 1). *RGLG1* expression is induced by ABA treatment and is markedly higher than *RGLG5* in seedlings (Supplemental Figure 2), which might explain the failure to

recover RGLG5 peptides. However, both *RGLG1* and *RGLG5* expression was induced to similar levels by cold, osmotic or salt stress in root (Supplemental Figure 2), which suggests that both genes play a relevant role in this tissue.

We employed additional strategies to confirm the PP2CA-RGLG1 interaction detected by Y2H and coIP/MS analysis and to further study the interaction of RGLG5 with PP2CA. Firstly, PP2CA interaction with RGLG1 and RGLG5 was confirmed by pull-down assays using recombinant purified proteins (Figure 1D). These *in vitro* assays were performed in the absence of ABA and revealed a basal affinity of PP2CA for RGLG1 and RGLG5. Then, to test whether they associate in plant cells, PP2CA and RGLG1 or RGLG5 were fused to the N-terminal fragment of LUC (nLUC-PP2CA) and the C-terminal fragment of LUC (RGLG1-cLUC or RGLG5-cLUC), respectively, and coexpressed in *Nicotiana benthamiana*. Compared to the negative control that expressed only nLUC-PP2CA+cLUC or nLUC+RGLG1/5-cLUC, RGLG1 and RGLG5 showed interaction with PP2CA in the absence of exogenous ABA addition, but after ABA supplementation, this interaction was markedly enhanced, suggesting ABA favored PP2CA-RGLG1 and PP2CA-RGLG5 interaction *in planta* (Figure 1E).

Although *in vitro* interaction of RGLG1/RGLG5 and PP2CA does not require exogenous ABA addition, results obtained *in planta* suggest that additional plant components might be involved in the enhanced ABA-dependent interaction observed in LUC assays. To further substantiate this concept, when GUS-tagged PP2CA was coexpressed with either GFP-tagged RGLG1 or FLAG-tagged RGLG5 in *N.benthamiana*, co-immunoprecipitation (coIP) assays indicated that in the absence of ABA, the interaction was weak, but it was dramatically enhanced by incubating the protein extracts with 10 μM ABA during coIP (Figure 1F). Similar results were obtained after testing their interaction with ABI2 and HAB2 (Figures 2B and 2C), which suggests that RGLG1 and RGLG5 might target several clade A PP2Cs in an ABA-dependent manner. Altogether, our data suggest that in *planta* interaction of the E3 ligases RGLG1 and RGLG5 with some clade A PP2Cs is strongly enhanced by

ABA.

Loss of function of RGLG1 and RGLG5 represses ABA-mediated responses

The above described interactions suggest potential roles of RGLG1 and RGLG5 in the ABA pathway as regulators of some clade A PP2Cs. Since these PP2Cs are key negative regulator of ABA signaling and a potential target of these E3 ligases, we predicted that impaired or enhanced expression of *RGLG1/5* might affect ABA signaling. Thus, to test whether RGLG1 and RGLG5 modulate ABA-mediated responses, loss-of-function mutants and overexpressing (OX) lines were used. *rglg1* was kindly provided by Dr. Bachmair (Yin et al., 2007), but for *RGLG5*, we could not confirm T-DNA insertion in several lines requested from public stock centers (Salk_021379 and CS812692 from ABRC, and 751D11 from MPIZ) and gene expression analyses indicated *RGLG5* transcript level was not decreased in these lines. Therefore, we generated knock-down mutant lines of *RGLG5* by designing a 35S artificial microRNA construct (Supplemental Figure 3A). Transcript level of *RGLG5* in several lines was examined by real-time PCR and we selected two lines (#2 and #4) whose *RGLG5* expression was below 20% of wild-type (wt), whereas expression of *RGLG1-4* was not significantly affected (Supplemental Figures 3B and 3C). We generated an *rglg1 amiR-rglg5* double mutant and several ABA-mediated responses, including inhibition of seed germination, seedling establishment and root growth were analyzed in *rglg1 amiR-rglg5* compared to other genetic backgrounds (Figures 3A-E). The well-studied *pp2ca-1* and *pyr1 pyl1 pyl2 pyl4* (*1124*) mutants served as internal controls of ABA-hypersensitive and ABA-insensitive phenotypes, respectively, and demonstrated the effectiveness of the ABA treatment (Kuhn et al., 2006; Yoshida et al., 2006; Park et al., 2009). None of the single *rglg1* or *amiR-rglg5* mutants had obvious differences in the above described ABA responses compared to wt (Figures 3A-E). However, the *rglg1 amiR-rglg5* double mutant, showed diminished ABA sensitivity compared to wt, suggesting partial functional redundancy of RGLG1 and RGLG5 in ABA-mediated responses.

Adult plants of wt, single *rglg1* or *amiR-rglg5* and *rglg1 amiR-rglg5* double

mutant were grown under well watered conditions and no obvious growth differences were observed among them (Supplemental Figure 3D). However, detached leaves of *rglg1 amiR-rglg5* showed higher water loss compared to wild-type or single mutants and under drought stress conditions the *rglg1 amiR-rglg5* double mutant showed reduced survival (Figures 4A-C), which is in agreement with its reduced ABA sensitivity. Conversely, the overexpression of either *RGLG1* or *RGLG5* reduced water loss and enhanced markedly plant survival under drought stress compared to wt (Figures 4D-F). Overexpression of either *RGLG1* or *RGLG5* led to enhanced ABA sensitivity in seed germination, seedling establishment and root growth assays, and increased ABA response under NaCl stress compared to wt (Supplemental Figures 4A-F). Finally, the induction of several ABA-responsive genes, including *RD29b* (Nordin et al., 1993), *RD22* (Abe et al., 2003), *RAB18* (Lang and Palva, 1992) and *P5CS1* (Strizhov et al., 1997), was diminished by down regulation of both *RGLG1* and *RGLG5* (Figure 3E), while enhanced by *RGLG1* and *RGLG5* overexpression (Supplemental Figure 4G). Altogether, these data demonstrate both RGLG1 and RGLG5 are positive regulators of ABA signaling in different ABA-mediated responses.

RGLG1 and RGLG5 mediate ubiquitination of the repressor PP2CA *in vitro*

Since not all RING-domain proteins possess E3 ligase activity (Deshaies and Joazeiro, 2009), it was important to determine whether RGLG5 has indeed ubiquitin ligase activity. Using purified GST-RGLG5, we showed RGLG5 could target itself for ubiquitination and the intensity of the ubiquitination band could be enhanced by increasing the reaction time (Supplemental Figure 5A). Moreover, RGLG5 self-ubiquitination was abolished either by the lack of any component of the ubiquitination reaction or by mutating (H406Y) or deleting the RING domain (Supplemental Figure 5B). Self-ubiquitination of RGLG1 was also confirmed in subsequent experiments (for instance Supplemental Figure 5C, panel anti-MBP). Then we asked whether RGLG1 and RGLG5 could directly target PP2CA for ubiquitination. Purified MBP-RGLG1 and MBP-RGLG5 were incubated with

GST-PP2CA in presence of all the other ubiquitination components. As a result, ubiquitination of PP2CA was promoted by MBP-RGLG1 and MBP-RGLG5 in a dose-dependent manner (Figures 5A and 5B; Supplemental Figure 5C), whereas lack of any component of the reaction abolished PP2CA ubiquitination (Figures 5A and 5B; Supplemental Figure 5C). Therefore both RGLG1 and RGLG5 promoted ubiquitination of PP2CA *in vitro*, whereas RING domain-mutated forms of RGLG1 (H462Y) and RGLG5 (H406Y) lost the ability to promote PP2CA ubiquitination (Figure 5C). Similar results were obtained after incubating ABI2 or HAB2 with these two RGLGs (Figures 5D-F). Taken together, these data indicate PP2CA as well as ABI2 and HAB2 can be ubiquitinated *in vitro* by the E3 ligases RGLG1 and RGLG5.

Since the *in planta* interaction of the E3 ligases RGLG1 and RGLG5 with PP2CA is strongly enhanced by ABA (Figure 1E), we investigated whether ABA or the ABA receptor PYL4 could modify in vitro ubiquitination of PP2CA (Supplemental Figure 6). In vitro ubiquitination of GST-PP2CA was not affected by the addition of ABA, PYL4 or both (Supplemental Figure 6). This result confirms the basal affinity of RGLG1 and RGLG5 for PP2CA and it suggests that either additional plant components, changes in their subcellular location or protein levels induced by ABA (for instance ABA-induced upregulation of *PP2CA* transcripts), might influence the interaction of PP2CA and RGLG1/RGLG5 in vivo.

PP2CA is subjected to 26S proteasome degradation and ABA enhances PP2CA degradation

The ubiquitination of PP2CA promoted by RGLG1 and RGLG5 might induce its degradation via the 26S proteasome. In spite of its key role in ABA signaling, protein levels and stability of PP2CA have not been investigated previously. It is well known that ABA induces transcriptional upregulation of clade A PP2Cs (Santiago et al., 2009; Fujita et al., 2009; Szostkiewicz et al., 2010; Supplemental Figure 7) and recent results from Kong et al., (2015) confirmed that ABI1 protein level is strongly increased by a 6 h ABA treatment. Since clade A PP2Cs are key negative regulators of ABA signaling, their ABA-mediated upregulation acts as a negative feedback

mechanism to reset and desensitize ABA signaling (Santiago et al., 2009). Both GUS histochemical staining and immunoblot analysis revealed a low expression of the *PP2CA* promoter in the absence of ABA which was markedly upregulated both in leaf and root tissues upon ABA treatment (Supplemental Figure 7A and 7B). This might generate difficulties to detect endogenous PP2CA under normal growth conditions and, additionally, the expected molecular weight of PP2CA is close to the Rubisco large subunit. We generated a PP2CA polyclonal antibody using truncated (1-200 amino acid residues) PP2CA as antigen to immunize rabbit and by immunoblot analysis we could detect PP2CA in etiolated seedlings (see Supplemental Figure 8 for PP2CA antibody specificity). We found that ABA treatment upregulated PP2CA protein level, which is in agreement with the upregulation of *PP2CA* transcripts and activation of *PP2CA* promoter (Supplemental Figures 7 and 8). To investigate PP2CA protein dynamics, we analyzed endogenous PP2CA levels in mock-, CHX- and CHX+MG132-treated seedlings (Figures 6A and 6B). These experiments revealed a turnover of PP2CA mediated by the 26S proteasome pathway. Next, we compared PP2CA protein stability in CHX-treated seedlings in the absence or presence of exogenous ABA. ABA treatment, in the absence of protein synthesis, enhanced PP2CA degradation (Figures 6C and 6D). Addition of the proteasome inhibitor MG132 blocked PP2CA degradation, which indicated that ABA-enhanced PP2CA degradation also occurs in the 26S proteasome (Figures 6E and 6F).

In order to avoid the use of CHX previously to ABA-treatment, which was required above to prevent ABA-mediated upregulation of the *PP2CA* promoter, we took advantage of *$35S_{pro}$:FLAG-PP2CA* transgenic lines. Direct measurements of PP2CA protein levels by western blot analysis showed ABA stimulated PP2CA degradation via the 26S proteasome pathway, since co-incubation with MG132 prevented this effect (Figures 6G and 6H). Similar results were obtained in a GUS activity assay using *Arabidopsis* protein extracts prepared from *$35S_{pro}$:PP2CA-GUS* transgenic lines submitted to different treatments (Figure 6I; Supplemental Figure 9). Moreover, we also generated *$35S_{pro}$:HA-PP2CA* lines in *pp2ca-1* background and

protein stability studies also indicated ABA-enhanced degradation of PP2CA, while continuous synthesis of PP2CA in the absence of degradation led to accumulation of the protein (Figures 6J and 6K). Taken together, these results reveal the turnover of PP2CA through the 26S proteasome, which is enhanced by ABA. Finally, we set up an *in vitro* cell-free degradation assay using purified His-PP2CA. We also found that degradation of His-PP2CA was enhanced by exogenous addition of ABA compared to mock-treated plants, which was attenuated by adding MG132 (Figures 6L and 6M).

RGLG1 and RGLG5 mediate ABA-dependent PP2CA degradation

To determine whether RGLG1 and RGLG5 mediate protein turnover of PP2CA, endogenous PP2CA protein levels were compared in wt and *rglg1 amiR-rglg5* seedlings that were treated with CHX in the absence or presence of exogenous ABA. The turnover of PP2CA was markedly diminished in *rglg1 amiR-rglg5* compared to wt, either in the absence or presence of exogenous ABA; therefore, RGLG1 and RGLG5 mediate PP2CA degradation (Figures 7A and 7B). To avoid the use of CHX together with ABA-treatment, protein dynamics of FLAG-PP2CA expressed in *rglg1 amiR-rglg5* was compared to that in wt (Figure 7C). ABA-promoted PP2CA degradation was abolished by down-regulation of the two *RGLG*s (Figure 7C and 7D). Conversely, ABA-enhanced degradation of FLAG-PP2CA in RGLG1ox or RGLG5ox plants was increased (Supplemental Figure 10A and 10B), suggesting that degradation of PP2CA in response to ABA is dependent on RGLG1 and RGLG5 function. We also conducted *in vitro* cell-free degradation assays by monitoring the level of His-PP2CA after incubation with protein extracts prepared from *rglg1 amiR-rglg5*, *RGLG1ox*, *RGLG5ox* or wt. Protein extracts prepared from *rglg1 amiR-rglg5* mitigated ABA's effect on stability of purified His-PP2CA (Figure 7E and 7F), whereas overexpression of *RGLG1* or *RGLG5* in these extracts enhanced the degradative effect of ABA on PP2CA (Supplemental Figure 10C-F). Addition of MG132 mitigated PP2CA degradation; however, MG132-resistant vacuolar proteases are released in cell-free degradation assays, which might explain the partial effect of this compound to

preserve PP2CA protein levels (Figure 7G and 7H; Supplemental Figure 10C-F).

Finally, we investigated whether RGLG1 and RGLG5 mediate PP2CA ubiquitination *in planta*. FLAG-tagged PP2CA either from wild type or *rglg1 amiR-rglg5* was separately immunoprecipitated after mock- or ABA-treatment, in presence of MG132. No obvious difference of FLAG-PP2CA ubiquitination level was observed in *rglg1 amiR-rglg5* after treatment with ABA while addition of exogenous ABA could increase the level of ubiquitinated PP2CA in Col-0 (Figure 7I). This result suggests RGLG1 and RGLG5 are required for ABA-promoted ubiquitination of PP2CA *in planta*. Altogether, the above data support RGLG1 and RGLG5 contribute to *in vivo* degradation of PP2CA.

Functions of RGLG1 and RGLG5 in ABA signaling are dependent on PP2CA

To determine the genetic relationship between *RGLG1/5* and *PP2CA*, we crossed the *pp2ca-1* loss-of-function mutant to *rglg1 amiR-rglg5* mutant. Since our results support that RGLG1/5 positively regulate ABA signaling by targeting PP2CA for degradation, *RGLG1/5* should act genetically upstream of *PP2CA*, and *pp2ca* loss-of-function mutant should attenuate or abolish some ABA-insensitive phenotypes of *rglg1 amiR-rglg5* mutant. *PP2CA/AHG3* encodes a phosphatase that strongly blocks ABA signaling during germination and *pp2ca-1* shows the strongest ABA-hypersensitivity in seed germination assays among loss-of-function mutants of clade A PP2Cs (Yoshida et al., 2006; Rubio et al., 2009). Therefore, we analyzed ABA-mediated inhibition of seed germination and seedling establishment in the *pp2ca-1 rglg1 amiR-rglg5* triple mutant since PP2CA plays a predominant role in this ABA response, whereas other putative PP2C targets -HAB2 or ABI2- play less relevant roles in this assay. As shown in Figure 8, ABA-mediated inhibition of radicle emergence, seedling establishment or early seedling growth in the triple mutant became similar to that of *pp2ca-1*, reflecting full recovery of ABA sensitivity in *rglg1 amiR-RGLG5* by *pp2ca-1*. This genetic analysis confirms a functional link between RGLG1/5 and PP2CA and indicates that RGLG1/5 act upstream of PP2CA in the ABA signaling pathway.

354

355

DISCUSSION

The "ABA-PYR/PYL/RCARs-PP2Cs-SnRK2s" core ABA signaling pathway has been widely studied in the past years and ABA-dependent PYR/PYL-mediated inhibition of PP2Cs has been extensively documented (Cutler et al., 2010; Finkelstein, 2013). Our work, together with recent results from Kong et al., (2015), unveils a second level of regulation during ABA signaling, i.e. the effect of ABA on PP2C protein levels. In our study we provide evidence that RGLG1/5 E3 ubiquitin ligases positively regulate various ABA responses by targeting PP2CA for degradation in the presence of ABA. In addition to PP2CA, we also found that HAB2 and ABI2 are candidate targets of RGLG1/5. Thus, ABA promoted the interaction of RGLG1/5 with HAB2 and ABI2 *in vivo* (Figures 2B and 2C), RGLG1/5 mediated ubiquitination of HAB2 and ABI2 *in vitro* (Figures 5D-F), and HAB2 was subjected to ABA-mediated degradation via the 26S proteasome pathway (Supplemental Figure 9). The recent report from Kong et al., (2015) has described the 26S proteasome degradation of the ABI1 PP2C mediated by PUB12/13 U-box E3 ligases, which belong to a different E3 family. In this latter case, only ABI1 was targeted for degradation by PUB12/13 ligases, whereas other PP2Cs closely related to ABI1 were not recognized by these E3 ligases. Therefore it seems RGLG1/5 might play a more general function in ABA pathway by regulating more than one PP2C. Another key difference between PUB12/13 and RGLG1/5 is that ubiquitination of ABI1 was absolutely dependent on the presence of ABA receptors whereas PP2CA, HAB2 and ABI2 were ubiquitinated in the absence of ABA receptors (Figure 5). This suggests the conformation of PP2CA, HAB2 and ABI2 allows their ubiquitination *in vitro* by RGLG1/5; however, we found that ABA somehow enhances PP2C-RGLG1/5 interaction *in vivo*, increasing the efficiency of ubiquitination and subsequent degradation. Altogether these studies reveal that both inhibition and degradation of clade A PP2Cs are important for activation of ABA signaling. Moreover, since degradation of ABI1 (Kong et al., 2015) and PP2CA (this work) was ABA-dependent, the role of PYR/PYL ABA receptors might extend beyond of reversible inhibition of the PP2Cs. Finally, the

385 ABA-insensitive phenotype of *rglg1 amiR-rglg5* is not as strong as that of *pyr/pyl*
386 combined mutants (Gonzalez-Guzman et al., 2012), which suggests that ABA
387 signaling can occur through inhibition of PP2C activity even in the absence of PP2CA
388 ubiquitination. However, since the *rglg1 amiR-rglg5* mutant shows reduced ABA
389 sensitivity even in the presence of a full set of PYR/PYLs, it suggests that PP2C
390 degradation is required for full activation of ABA signaling.

391 Whereas inhibition of PP2C activity is a reversible mechanism that regulates
392 ABA signaling according to fluctuating ABA levels in response to environmental cues,
393 degradation of PP2C is an irreversible decision that could lead to sustained ABA
394 signaling when stress situation persists. Ubiquitination of PP2Cs might be reversed by
395 deubiquitinating enzymes, providing an additional source of regulation on protein
396 stability from core ABA signaling components (Zhao et al., 2016). In nature, both
397 transient and sustained forms of stress occur; therefore, a double mechanism to
398 abolish PP2C function seems to be better prepared to cope with different
399 environmental stresses. In this way, monitoring the repressor protein abundance
400 provides an additional mechanism to regulate ABA signaling, which complements the
401 biochemical inhibition of phosphatase activity through PYR/PYLs. Thus, ABA, as
402 other hormones such as auxin, jasmonate and gibberellin, follows a relief of
403 repression mechanism that degrades negative regulators via 26S proteasome (Santner
404 and Estelle, 2010; Kelley and Estelle, 2012; Kong et al., 2015). A model integrating
405 RGLG1/5 into the ABA signaling pathway is shown in Figure 9, where
406 RGLG-mediated PP2CA degradation could be auxiliary to PYR/PYL-mediated
407 inhibition of PP2CA activity. This model illustrates the idea that ubiquitin-mediated
408 degradation of the PP2CA repressor might be dependent on ABA perception or
409 facilitated by the upregulation of *PP2CA* transcripts induced by ABA. In the first case,
410 the ABA-Receptor-PP2CA ternary complex, in addition to inhibiting PP2CA activity,
411 might label PP2CA for degradation. Alternatively, RGLG1/5-PP2CA interaction
412 might be simply facilitated by the higher PP2CA protein level induced by
413 upregulation of *PP2CA* transcripts. Paradoxically, whereas ABA inhibits PP2C

activity through ABA receptors and promotes ABI1 and PP2CA degradation, it also up-regulates *ABI1* and *PP2CA* transcripts as a feedback mechanism. The role of the 26S proteasome in the turnover of PP2Cs (Kong et al., 2015, this work) and ABA receptors (Bueso et al., 2014; Irigoyen et al., 2014) is further extended by the observation that ZmOST1 seems to be targeted for proteasome degradation by casein kinase 2-mediated phosphorylation at the ABA box (Vilela et al., 2015).

METHODS

PP2CA polyclonal antibodies and immunoblot detection of endogenous PP2CA

The polyclonal antibody of PP2CA was generated by Shanghai ImmunoGen Biological Technology Co., Ltd (ABclonal). To avoid cross reaction with other PP2Cs, a fragment of truncated PP2CA (1-200 amino acids) was fused with GST tag and the recombinant protein expressed in E. coli was used as an antigen to raise polyclonal antibody in rabbit. The resulting antiserum was purified by IgG-affinity chromatography. To ensure specific binding to PP2CA, the antibody was further isolated by membrane strip affinity purification. Briefly, 200 μg purified His-PP2CA was loaded into a SDS-PAGE gel and then transferred to Nitrocellulose membrane. The membrane containing His-PP2CA was stained with Ponceau S solution and cut into small strip. The strip was pre-eluted with 2 ml 0.2 M glycine (pH 2.7) for 2 min and then blocked with 5% non-fat milk in TBST for 1 h. After washing the membrane with TBST for three times, it was incubated with antibody solution (200 μl antibody in 3 ml TBS) overnight and then washed again with TBST for 3 times. The antibody was eluted by incubating with 100-200 μl 0.2 M glycine (pH 2.7) for 2 min. The resulting antibody solution was neutralized with 2 M Tris-HCl (pH 8.5), generating a final concentration of 150 mM Tris-HCl. The elution and neutralization steps were repeated for two more times. The final antibody solution was dialyzed against 1×PBS (pH 7.4), concentrated to a volume of 150 μl with ultra-filtration column, and tested by western blot analysis. To prepare protein extracts, seedlings were grown vertically on MS solid medium under dark condition for 2 weeks and then transferred into liquid MS medium supplemented with different chemicals under dark condition for the indicated time points. Samples were harvested and total proteins were extracted by homogenizing the seedlings in the lysis buffer (50 mM Tris-HCl, pH 7.5, 150 mM NaCl, 0.1% NP-40, 1 mM DTT, 1mM PMSF and plant-specific protease inhibitor cocktail) at a ratio of 1:2 (m/v). The concentration of total protein was determined by Bradford assays and equal amount of total proteins were mixed with 4×SDS loading

buffer. Boiled samples were separated by SDS-PAGE gel electrophoresis and analyzed by western blot. The polyclonal antibody of PP2CA α-E2663 was used to detect endogenous PP2CA protein levels. Actin was detected as loading control.

Plant materials and growth condition

Arabidopsis thaliana ecotype Col-0 was used as wild type. *rglg1* (SALK_062384) mutant was requested from Dr. Andreas Bachmair. *RGLG5* knock-down mutants were generated based on artificial microRNAs strategy. Seeds of *pyr1 pyl1 pyl2 pyl4* (*1124*) were requested from Dr. Sean R. Cutler. Seeds of *pp2ca-1* were kindly provided by Dr. Julian I Schroeder; ABI2-GFP transgenic seeds were gifted by Dr. Dapeng Zhang. *Arabidopsis* plants were grown as previously described (Zhang et al., 2012). *N.benthamiana* plants were grown under a 16 h/8 h photoperiod.

Knock down of *RGLG5* by artificial microRNA-based strategy

Overlapping PCR was performed using specific primers designed by Web MicroRNA Designer (http://wmd3.weigelworld.org/cgi-bin/webapp.cgi) and plasmid pBSK as template to replace miR319a sequence by a 21 nucleotides sequence "GTCGTTCACTTATAGGAAACT" designed to target *RGLG5* transcript. After verification by sequencing, the amiRNA precursor was digested with XhoI/SpeI, and cloned into pJim19 digested with the same restriction enzymes. The constructs were introduced into *Agrobacterium tumefaciens* strain EHA105 by electroporation, and the wild-type plants were transformed using the floral dip method as reported previously (Clough and Bent, 1998). Seeds of the transformed plants were selected by hygromycin. Homozygous T3 transgenic seeds or plants were used for further studies. To obtain *rglg1 amiR-rglg5* double mutant, homozygous *rglg1* was crossed with *amiR-rglg5* (4#). Seeds were sowed on MS medium containing 25 μg/ml hygromycin and T-DNA insertion in *rglg1* was confirmed by PCR using primers LBa1 and 323A, genomic DNA as template.

Generation of transgenic plants

RGLG1, *RGLG5* and *PP2CA* cDNAs were each cloned into XhoI/SpeI- digested pJim19, resulting in a fusion with 3× FLAG tag at the N terminus. To construct *RGLG1-GFP* and *RGLG5-GFP*, the *GUS* sequence of pBI121 was replaced by *GFP* cDNA via Bam HI/SacI sites. The *pBI121-RGLG1-GFP* and *pBI121-RGLG1-GFP* plasmids were then created by linking *RGLG1* or *RGLG5* coding region without stop codon to the *GFP* (C terminus) via Bam HI and KpnI. To construct *PP2CA-GUS* and *HAB2-GUS* fusions, entire coding sequences of *PP2CA* and *HAB2* with no stop codons were amplified by PCR and separately inserted into pBI121-GUS vector upstream of GUS. The primers used above are given in Supplemental Table 2. All the constructs are under the control of CaMV 35S promoter. These constructs were introduced into *Agrobacterium tumefaciens* strain EHA105 by electroporation, and the wild-type or mutant plants were transformed using the floral dip method as reported previously (Clough and Bent, 1998). Seeds of the transformed plants were selected by hygromycin for pJIM19 constructs or kanamycin for pBI121 constructs. Homozygous T3 transgenic seeds or plants were used for further studies. The generation of *$35S_{pro}$:3HA-PP2CA* transgenic lines in *pp2ca-1* background was performed as described (Antoni et al., 2012). Transgenic *Arabidopsis FLAG-PP2CA×RGLG1-GFP* and *FLAG-PP2CA×RGLG5-GFP* were obtained by crossing *FLAG-PP2CA* with either *RGLG1-GFP* or *RGLG5-GFP* transgenic lines. Transgenic *Arabidopsis ABI2-GFP×FLAG-RGLG1* or *ABI2-GFP×FLAG-RGLG5* was produced by crossing *ABI2-GFP* with *FLAG-RGLG1* or *FLAG-RGLG5* transgenic lines, respectively.

To construct the *$PP2CA_{pro}$:GUS* gene, a fragment comprising 2 Kb 5' upstream of the ATG start codon from *PP2CA* was amplified by PCR using the following primers: FproPP2CA (5'-**AAG CTT** GGT TTT ACC CGA ACT TAA CCC AAA TGC-3', including HindIII site) and RproPP2CA (5'-**GAG CTC** CAT TTG ATC TCT AAC AAA ACT TCT CCA-3', including SacI site). The PCR product was cloned into

511 pCR8/GW/TOPO. Next, it was recombined by Gateway LR reaction into pMDC163
512 destination vector (Curtis and Grossniklaus, 2003), in-frame with the *GUS* gene. The
513 pMDC163-based construct carrying the *PP2CA*$_{pro}$*:GUS* gene was transferred to
514 *Agrobacterium tumefaciens* pGV2260 (Deblaere et al., 1985) by electroporation and
515 used to transform Col-0 wild-type plants by the floral dipping method (Clough and
516 Bent, 1998). Seeds of transformed plants were harvested and plated on hygromycin
517 (20 μg/ml) selection medium to identify T1 transgenic plants, and T3 progenies
518 homozygous for the selection marker were used for further studies. Imaging of GUS
519 was performed as previously described (Gonzalez-Guzman et al., 2012).

520 **Yeast two hybrid assay**

521 *RGLGs* were cloned into pGBKT7 vector as bait and *PP2Cs* were inserted into
522 pGADT7-Rec vector as prey, respectively. For interaction assays, each pair of bait and
523 prey constructs were cotransformed into yeast strain AH109 based on the
524 manufacturer's instructions of the MatchMaker GAL4 Two-Hybrid System (Clontech).
525 Transformants growing well on SD/-Leu/-Trp medium were taken as positive clones
526 harboring both plasmids. Interactions between two proteins were determined by
527 growing transformants on SD/-Leu/-Trp/-His/-Ade medium with serial dilution and
528 quantifying β-galactosidase activities using o-nitrophenyl-β-D-galactopyranoside
529 (Sigma) as substrate. Yeast protein extracts were analyzed by immunoblotting using
530 anti-HA antibody to detect PP2C proteins fused to the GAL4 activation domain (AD)
531 and anti-myc antibody to detect RGLG proteins fused to the GAL4 DNA binding
532 domain (BD) according to manufacturer's instructions (Clontech).

533 **Firefly luciferase complementation imaging assay (LCI)**

534 The full-length *PP2CA* was fused upstream of N-*Luc* in the pCAMBIA1300-NLuc
535 vector, and *RGLG1* or *RGLG5* was fused downstream of C-*Luc* in the
536 pCAMBIA1300-CLuc vector. The resulting constructs were transferred into
537 *Agrobacterium tumefaciens* strain EHA105. To determine the interaction between
538 PP2CA and RGLG1 or RGLG5, *Agrobacterium* harboring the indicated vectors were

resuspended in infiltration buffer containing 10 mM $MgCl_2$, 10 mM MES, 0.5 g/l glucose and 150 μM acetosyringone to a final concentration of OD_{600} = 0.5. Equal volumes of different combinations were mixed and co-infiltrated into *Nicotiana benthamiana* leaves using a needleless syringe. Plants were first kept under dark for 24 h, and then at 16 h light/8 h dark for another 24-48 h at 22℃. MG132 was infiltrated into the same region 12 h before inspection. To test the effects of ABA treatment, 50 μM ABA was infiltrated into the same area on leaves 3 h before observation. *N.benthamiana* leaves were infiltrated with 0.1 mg/ml luciferin and placed under dark for 5 min before CCD imaging. LUC activity was observed with a low-light cooled CCD imaging apparatus (Berthold Technologies). The exposure time of LUC was 1-10 min depending on the signal intensity.

Expression and purification of recombinant protein

Full length *RGLG5*, *PP2CA*, *HAB2* and *ABI2* coding sequences were amplified by PCR and cloned into the prokaryotic expression vector pGEX-4T-1 (Amersham Biosciences) to generate GST fusions. To produce MBP fusion proteins, the full length coding regions of *RGLG1* and *RGLG5* were amplified and cloned into pMAL-c2x vector (New England Biolabs). Primers used are listed in Supplemental Table 2. QuikChange Lightning Multi Site-Directed Mutagenesis Kit (Agilent Technologies) was used to produce Ring-domain mutated form of RGLG1 (H462Y) and RGLG5 (H406Y) by PCR amplification with specific primers and indicated plasmid as template. Recombinant His-PP2CA was produced as described (Antoni et al., 2012). To generate His-PYL4, full length coding sequence of PYL4 was amplified, digested by *Eco*RI and *Xho*I, and inserted into pET-28a. The recombinant constructs were then transformed into *Escherichia coli* strain BL21 (DE3). For expression, 1 mM IPTG was added to the cell culture to induce GST-tagged proteins whereas 0.3 mM and 0.4 mM IPTG were needed to efficiently induce MBP and His fusion proteins, respectively. The soluble GST-tagged proteins were purified using the MagneGST™ protein purification system (Promega) according to the manufacturer's protocols. Purification of MBP fusion proteins was carried out following the

manufacturer's instructions of pMAL Protein Fusion and Purification System (New England Biolabs). The soluble His-fusion protein was extracted and immobilized onto Ni-NTA agarose beads (QIAGEN) and the purification procedures were conducted according to the protocols for purification under native conditions in the QIAexpressionist.

***In vitro* pull-down assay**

Equal amount of purified MBP, MBP-RGLG1 or MBP-RGLG5 proteins were incubated with equal volume of amylose resin beads (New England Biolabs) in buffer A1 containing 1×TBS, 1 mM PMSF, and protease inhibitor cocktail at 4℃ for two hours with gentle rotation. The beads were then washed three times with buffer A1 and aliquoted equally into four parts. The indicated amount of purified His-PP2CA of was added to the mixture, and incubated overnight at 4℃. After washing 5 times with buffer A2 containing 1×TBS, 1 mM PMSF, 0.05% Triton X-100 and protease inhibitor cocktail, the bound proteins were eluted with 1× SDS loading buffer with boiling for 5 min at 100℃ and examined by western blot using anti-His or anti-MBP antibodies.

Cell-free protein degradation assay

Cell-free protein degradation assay was conducted as previously described (Wang et al., 2009). Briefly, Seven-day-old Arabidopsis seedlings of different genotypes were harvested and grounded into fine powder in liquid nitrogen. Total proteins were extracted in the degradation buffer containing 25 mM Tris-HCl, pH 7.5, 10 mM NaCl, 10 mM $MgCl_2$, 4 mM PMSF, 5 mM DTT and 10 mM ATP. The debris was removed by two times of centrifugations at 16000 g for ten minutes at 4 °C and the supernatants were transferred to new tubes. Protein concentration was determined using the Bradford method (Biorad). Then, the total extracts of each genotype were adjusted to equal concentration with the degradation buffer. To monitor the degradation of the recombinant His-PP2CA protein, 100 ng of the purified protein was incubated in 100 μl total extracts (containing 500 μg total proteins) at 15 °C for

each assay. ABA and MG132 were added to the *in vitro* degradation assays as indicated. Reactions were stopped by adding 4×SDS loading buffer. Samples were taken at the indicated intervals to determine the abundance of the remained His-PP2CA by western blot using anti-His antibody (Bioeasy). The bands intensity was quantified using Image J software (http://imagej.nih.gov/ij/).

***In vitro* ubiquitination assay**

Self-ubiquitination assay was performed as described (Zhang et al., 2012) . For *in vitro* substrate ubiquitination assay, a total reaction volume of 30 μl was mixed by adding 500 ng purified MBP-RGLG1 (MBP-RGLG1H462Y) or MBP-RGLG5 (MBP-RGLG55H406Y), 300 ng GST-PP2CA or GST-HAB2 or GST-ABI2, 50 ng E1 (Sigma), 100 ng E2 UbcH5b (Enzo Life Sciences), 3 μg FLAG-tagged ubiquitin (Sigma), 10 mM phosphocreatine, and 0.1 unit of creatine kinase in the ubiquitination buffer (50 mM Tris-HCl pH 7.5, 3 mM ATP, 5 mM $MgCl_2$, and 0.5 mM DTT) and incubated at 37 °C for 2 h. The reaction was stopped by adding 4× SDS loading buffer. Samples were separated by 8% SDS-PAGE gel and analyzed by western blot using anti-GST (Abmart), anti-FLAG (Sigma) or anti-MBP (Earthox) antibody.

***In vivo* immunoprecipitation assays**

For coimmunoprecipitation using *ABI2-GFP×FLAG-RGLG1* or *ABI2-GFP×FLAG-RGLG5* transgenic *Arabidopsis*, 2-week-old seedlings were transferred from selective MS medium to liquid MS containing 50 μM ABA for the indicated time. ~300 mg plant materials were harvested and total proteins were extracted in 3 volumes of lysis buffer (50 mM Tris-HCl, pH 7.5, 100 mM NaCl, 0.1% NP-40, 50 μM MG132, 1 mM DTT, 1mM PMSF and plant-specific protease inhibitor cocktail). The concentration of total protein was determined by Bradford assays (Bio-Rad), and each lysate (1 ml) with equal amount of protein was immunoprecipitated by incubating with 20 μl anti-GFP mAb-Agarose (MBL) beads for 4 h at 4℃ with gentle rotation. For immunoprecipitation with anti-FLAG antibody, the lysates were incubated with 0.5 μl anti-FLAG and 25 μl Protein G-Sepharose (Invitrogen) beads for 4 h at 4℃ with gentle rotation. After incubation,

the beads were washed with 1 ml of lysis buffer for 4 times and eventually eluted by adding 30 μl 1× SDS protein loading buffer and boiling for 5 min at 100℃. Immunoprecipitated proteins were separated by 10% SDS-PAGE gel and checked using anti-FLAG or anti-GFP (Abmart) antibody.

For coimmunoprecipitation in *Nicotiana benthamiana*, 4- to 5-week-old *N.benthamiana* leaves were infiltrated with *Agrobacterium* harboring the indicated constructs. The agroinfiltration was performed as described above in "**Firefly luciferase complementation imaging assay**". 50 μM MG132 was also infiltrated into the same region 12 h before sample collection to inhibit protein degradation. Protein extracts were prepared as indicated above except that the lysates were incubated with or without 10 μM ABA at 4℃ for 3 h before immunoprecipitation. Polyclonal anti-GFP (1 mg/ml, MBL) or anti-FLAG antibody coupled with 25 μl Protein G-Sepharose was then added to immunoprecipitate the total protein extracts. As negative controls, IgG was added in parallel to eliminate non-specific binding. After elution as above, samples were subjected to western blot analysis, and anti-GUS (Sigma), anti-GFP or anti-FLAG antibody were used to detect fusion proteins.

To detect the ubiquitination form of PP2CA *in vivo*, 2-week-old transgenic Arabidopsis *35S:3×FLAG-PP2CA*/Col-0 and *35S:3×FLAG-PP2CA*/*rglg1 amiR-rglg5* were treated with MG132 or in combination of ABA for 6 h. Samples were harvested and total proteins were extracted as indicated above except that deubiquitinylating enzymes inhibitor PR619 (Sigma) were also included in the lysis buffer. The concentration of total proteins was determined by Bradford assays, and each lysate with equal amount of protein (500 mg) was immunoprecipitated by incubating with 0.5 μl anti-FLAG and 25 μl Protein G-Sepharose beads for 6 h at 4℃ with gentle rotation. Immunoprecipitated products were obtained as mentioned above and analyzed by immunoblots. Anti-FLAG antibody was used to detect total FLAG-PP2CA and anti-ubiquitin to detect the ubiqutinated PP2CA in plant.

IP-Mass Spectrometry analysis

2-week-old transgenic Arabidopsis seedlings overexpressing FLAG-PP2CA were

654 treated with 50 μM MG132 for 24 h and 50 μM ABA for 6 h. 4-5 g materials were
655 harvested for total protein extraction. Anti-FLAG immunoprecipitates were prepared
656 as described in "***In vivo* immunoprecipitation assays"**. FLAG-tagged proteins
657 were finally eluted from the beads by adding 400 μg/ml 3×FLAG peptides in 1×PBS
658 buffer, with gentle rotation at 4ºC for 1 h×3 times. The eluted proteins were then
659 collected and lyophilized. A final volume of 30 μl 1×PBS buffer was added to
660 resuspend the powder. The resulting products were resolved on 4-12% NuPAGE®
661 Bis-Tris MiNi Gel (Invitrogen) and visualized by colloidal blue staining kit
662 (Invitrogen). The protein bands from 15 to 100 KD were cut from the gel and digested
663 with trypsin. The extracted peptides were subjected to LC-MS/MS analysis using
664 Easy nLC 1000 system (Thermo Scientific) connected to a Velos Pro Orbitrap Elite
665 mass spectrometer (Thermo Scientific) equipped with a nano-ESI source. The raw
666 data files were converted to mascot generic format (".mgf") using MSConvert before
667 submitted for database search. Protein identification was carried using Mascot server
668 v. 2.3.02 (Matrix Science) against TAIR *Arabidopsis thaliana* protein database.

669 ***In vivo* protein degradation assay**

670 Seedlings were grown vertically on MS solid medium for 2 weeks and then
671 transferred in liquid MS medium supplemented with 50 μM ABA for the indicated
672 time points. Samples were harvested and total proteins were extracted by
673 homogenizing the seedlings in the lysis buffer containing 50 mM Tris-HCl, pH 7.5,
674 150 mM NaCl, 0.1% NP-40, 1 mM DTT, 1mM PMSF and plant-specific protease
675 inhibitor cocktail at a ratio of 2:1 (m/v). The concentration of total protein was
676 determined by Bradford assays and equal amount of total proteins were mixed with
677 2× SDS loading buffer. Boiled samples were separated by SDS-PAGE gel
678 electrophoresis and analyzed by western blot. Anti-FLAG was used to detect
679 FLAG-PP2CA and anti-GFP to confirm the expression of RGLG fusions. Anti-Actin
680 was detected as a loading control.

681 **GUS assays**

682 For protein stability analysis, transgenic *Arabidopsis* seedlings carrying
683 *pBI-PP2CA-GUS*, *pBI-HAB2-GUS* or *pBI-GUS* (negative control) were germinated

and grown on MS plate supplemented with 50 μg/ml kanamycin for 7 days followed by transferring to liquid MS medium with or without 50 μM MG132, and/or 100 μM cycloheximide (CHX, Sigma), as well as 50 μM ABA for the indicated time. Treated seedlings were collected for GUS staining, which was performed following the method described previously (Zhang et al., 2012) and stained plants were visualized using Leica E24HD. GUS activity was measured as reported recently (Zhang et al., 2015). Briefly, total protein was extracted from 7-day-old seedling tissues using GUS extraction buffer (50 mM sodium phosphate buffer, pH7.5, 10 mM β-mercaptoethanol, 0.1% Triton X-100 and 10 mM EDTA) followed by quantification by Bradford assays. Then 50 mg total protein was firstly incubated at 37°C for 5 min before 1 mM 4-Methylumbelliferyl-β-D-glucuronide (4-MUG) (Sigma) was added. After 60 min of reaction, 100 μl sample was taken and 2.4 ml 0.2 M Na_2CO_3 was added to terminate the reaction, then each sample was quantified for absorbance at Ex 365/Em 455 with a fluorospectrophotometer (Hitachi) to calculate 4-methylumbelliferone (4-MU) production. The final GUS activity was expressed as pmol (4-MU) · min^{-1} ·μg^{-1} (fresh weight).

Phenotype analysis

For germination assay, about 100 sterilized seeds of each genotype were sowed on MS plates supplemented without or with different concentrations of ABA. After stratification in the dark at 4℃for 3 days, plates were transferred to greenhouse at 22℃ under a 16 h/8 h photoperiod. Germination rate was the percentage of seeds that showed an obvious emergence of radicle after 3 days. Seedling establishment was scored after 7 days as the percentage of seedlings that developed fully green expanded cotyledons (Pizzio et al., 2013).

For root growth assay, seeds were grown vertically on MS medium for 3-5 days and then 10 seedlings of each genotype were transferred to MS plates in the presence or absence of different concentrations of ABA for another periods of time (Pizzio et al., 2013). Then photographs were taken and primary root length was monitored and analyzed using ImageJ software.

To study the effect of NaCl on germination and postgermination growth, seeds were sown on MS plates with or without various concentrations of NaCl and the plates were kept in the dark at 4ºC for 3 days. Afterward, the plates were moved to greenhouse under long-day conditions (16-h-light/8-h-dark cycle). Photographs were taken 7 days later to record different sensitivities to NaCl of each genotype.

To measure leaf water loss, rosette leaves of similar developmental stages from 4-week-old plants grown under short-day conditions (8-h-light/16-h-dark cycle) were excised from their roots, placed on open Petri dishes, and kept on the lab bench for the indicated time and then their fresh weights were monitored. Water loss was expressed as a percentage of weight loss at the indicated time versus initial fresh weight (Zhu et al., 2007). For drought treatment experiment, 7-day-old plants were transferred from MS medium to water-saturated soil and the plants were grown under short-day conditions until they were 3 weeks old. Watering was withdrawn until severe damage was observed in wt plants (18-20 d). Survival rate was recorded 3 days after rehydration (Zhu et al., 2007). To minimize experimental variations, the same numbers of plants were grown on the same tray.

RNA extraction and real-time PCR

For qRT-PCR analysis of ABA-responsive genes, 7-day-old seedlings grown under long-day conditions were transferred to liquid MS medium supplemented with or without 50 μM ABA for the indicated time. Total RNA extraction, cDNA synthesis and real-time PCR were performed as described (Zhang et al., 2012). UBQ10 was used as an internal control for normalization of transcript levels (Zhang et al., 2012). Primers used for gene expression analyses are listed in Supplemental Table 2.

Accession Numbers

The *Arabidopsis* Genome Initiative numbers for genes mentioned in this article are as follows: *RGLG1* (At3G01650), *RGLG2* (At5G14420), *RGLG3* (At5G63970), *RGLG4* (At1G79380), *RGLG5* (At1G67800), *ABI1* (AT4G26080), *ABI2* (AT5G57050), *PP2CA* (AT3G11410), *HAB1* (AT1G72770), *HAB2* (AT1G17550), *RD29a*

(AT5G52310), *RD29b* (AT5G52300), *RAB18* (AT5G66400), *RD22* (AT5G25610), *DREB2A* (AT5G05410), *P5CS1* (AT2G39800), *ERD10* (AT1G20450), *ADH1* (AT1G77120), *PYL4* (AT2G38310)

Supplemental Data

The following materials are available in the online version of this article.

Supplemental Figure 1. Immunoblot analysis verifies the expression of the AD-PP2Cs and BD-RGLGs proteins in the Y2H assay.

Supplemental Figure 2. Relative expression of *RGLG1* and *RGLG5* in seedlings.

Supplemental Figure 3. Generation of *RGLG5* knock-down lines by artificial microRNA strategy.

Supplemental Figure 4. ABA hypersensitivity in *Arabidopsis* transgenic lines overexpressing either *RGLG1* or *RGLG5*.

Supplemental Figure 5. E3 ligase activity of RGLG5 and *in vitro* ubiquitination of PP2CA by RGLG1 and RGLG5.

Supplemental Figure 6. *In vitro* ubiquitination of PP2CA by RGLG1 and RGLG5 is not affected by ABA and PYL4.

Supplemental Figure 7. Expression of the *PP2CA* promoter is strongly induced by ABA. Transcriptional profiles of *PP2C* genes in response to ABA.

Supplemental Figure 8. α-E2663 is an specific antibody for PP2CA. ABA up-regulates PP2CA protein level.

Supplemental Figure 9. GUS staining of seedlings expressing PP2CA-GUS or HAB2-GUS reveals ABA-induced degradation of the phosphatases via the 26S proteasome pathway.

Supplemental Figure 10. Overexpression of *RGLG1* or *RGLG5* enhances ABA-promoted degradation of FLAG-PP2CA.

Supplemental Table 1. List of peptides identified for PP2CA and RGLG1 in anti-FLAG immunoprecipitates obtained from $35S_{pro}$:3×FLAG-PP2CA Arabidopsis seedlings mock-treated or treated with ABA and MG132.

Supplemental Table 2. List of primers used in this study.

ACKNOWLEDGMENTS

We thank Dr. Andreas Bachmair for *rglg1* mutant, Dr. Sean R. Cutler for seeds of *pyr1 pyl1 pyl2 pyl4*, Dr. Dapeng Zhang for transgenic material of ABI2, Dr. Hongwei Guo and Dr. Jianmin Zhou for pCAMBIA1300-Nluc and pCAMBIA1300-Cluc vectors, Dr. John Olson for assistance in English editing. This work was supported by grants from the National Key Basic Science "973" Program (grant no. 2012CB114006) and the National Natural Science Foundation (grant nos. 31272023, 31170231 and 90817001) of the Chinese government. Work in the lab of P.L.R. was funded by grant BIO2014-52537-R from MINECO.

AUTHOR CONTRIBUTIONS

Q. W., X. Z., M.P-L., B.B-P., X. Y., C. A. and P.L.R. designed experiments; Q. W., X. Z., M.P-L., B.B-P., X. W. and S. C. performed the experiments; Q. W., X. Z., C. A. and P.L.R. wrote the manuscript; all authors discussed the results and commented on the manuscript.

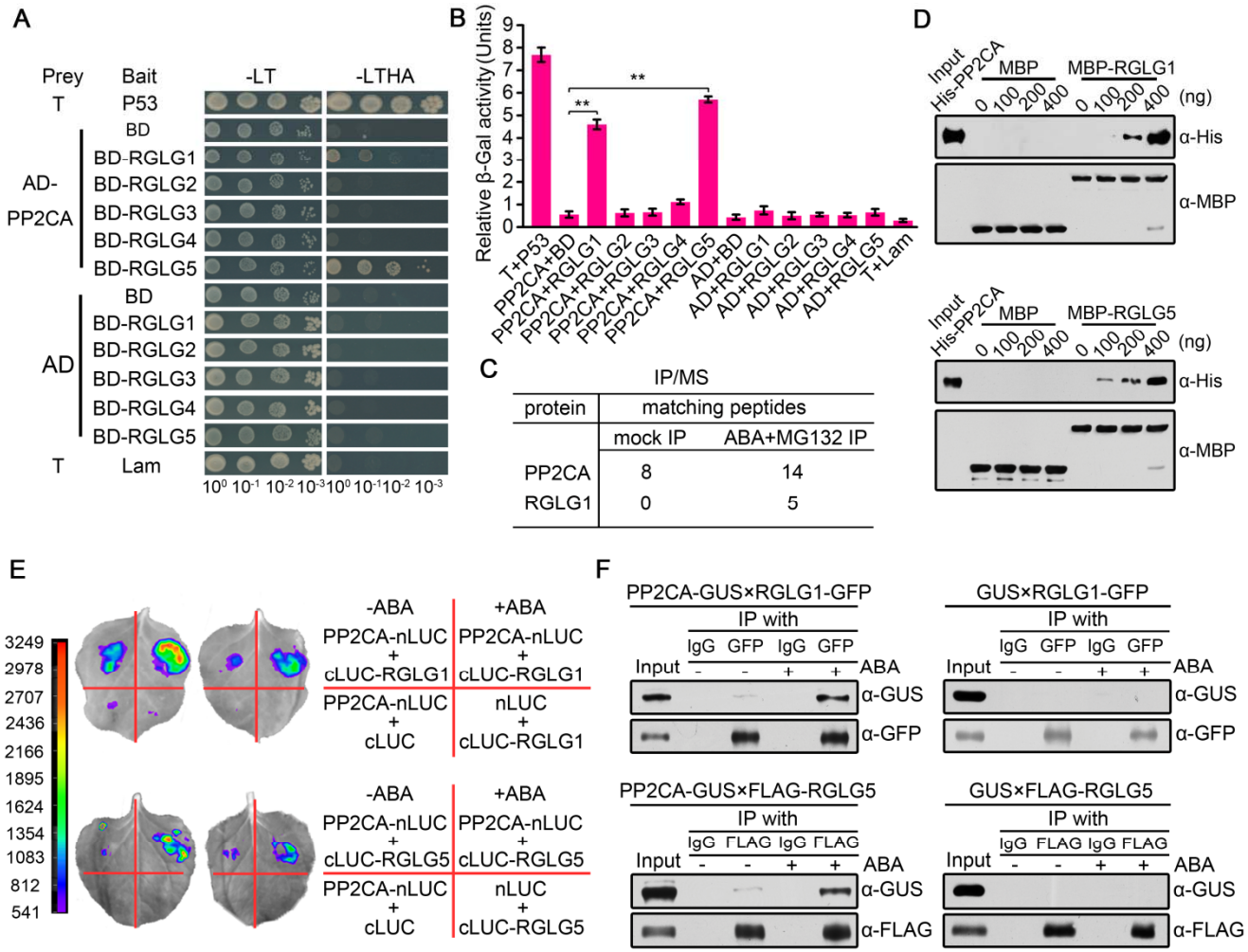

Figure 1. *In vitro* and *in vivo* interaction of PP2CA with ubiquitin ligases RGLG1 and RGLG5.
(A) Interaction of PP2CA with RGLGs in yeast two-hybrid assays. Photographs were taken 5 days after yeast cells were grown on Leu⁻ Trp⁻ /Yeast Nitrogen Base (YNB) or Leu⁻ Trp⁻ His⁻ Ade⁻/YNB medium. The T+Lam and T+P53 were used as negative and positive controls for the yeast two-hybrid system, respectively.
(B) Quantitative analysis of interactions in **(A)** by measuring β-galactosidase (β-gal) activities. o-nitrophenyl -β-D-galactopyranoside was used as substrate. Bars indicate the mean ± standard deviation (SD) from the three replicas. Asterisks indicate a significant difference from the negative control pair AD-PP2CA+BD (Student's t-test: **, $P < 0.01$).
(C) Number of PP2CA and RGLG peptides identified by IP/Mass Spectrometry (MS). Total proteins were extracted from seedlings of *35S$_{pro}$:3×FLAG-PP2CA* treated without (mock) or with ABA and MG132. Immunoprecipitation (IP) was performed using anti-FLAG and the IP products were analyzed by mass spectrometry.
(D) *In vitro* interaction of PP2CA with RGLG1 and RGLG5. Serial concentrations of His-tagged PP2CA were incubated with immobilized MBP-RGLG1, MBP-RGLG5 or MBP proteins. Bounded proteins were detected by western blot using anti-His and anti-MBP antibodies.
(E) Interaction between PP2CA and RGLG1 or RGLG5 in firefly luciferase complementation imaging assay. Construct pairs PP2CA-nLUC/ RGLGs-cLUC, PP2CA-nLUC/cLUC, nLUC/ RGLGs-cLUC were co-expressed in *N. benthamiana* leaves. 50 μM ABA was injected 3 h before LUC observation. Two representative results were shown.
(F) Coimmunoprecipitation of PP2CA with RGLG1 and RGLG5. GUS-tagged PP2CA and GFP-tagged RGLG1 or FLAG-tagged RGLG5 were co-expressed in *N. benthamiana*. Protein extracts were incubated with (+) or without (-) 10 μM ABA for 3 h before immunoprecipitation using GFP or FLAG antibodies bounded to Protein G-Sepharose beads. IgG was added in parallel as negative controls.

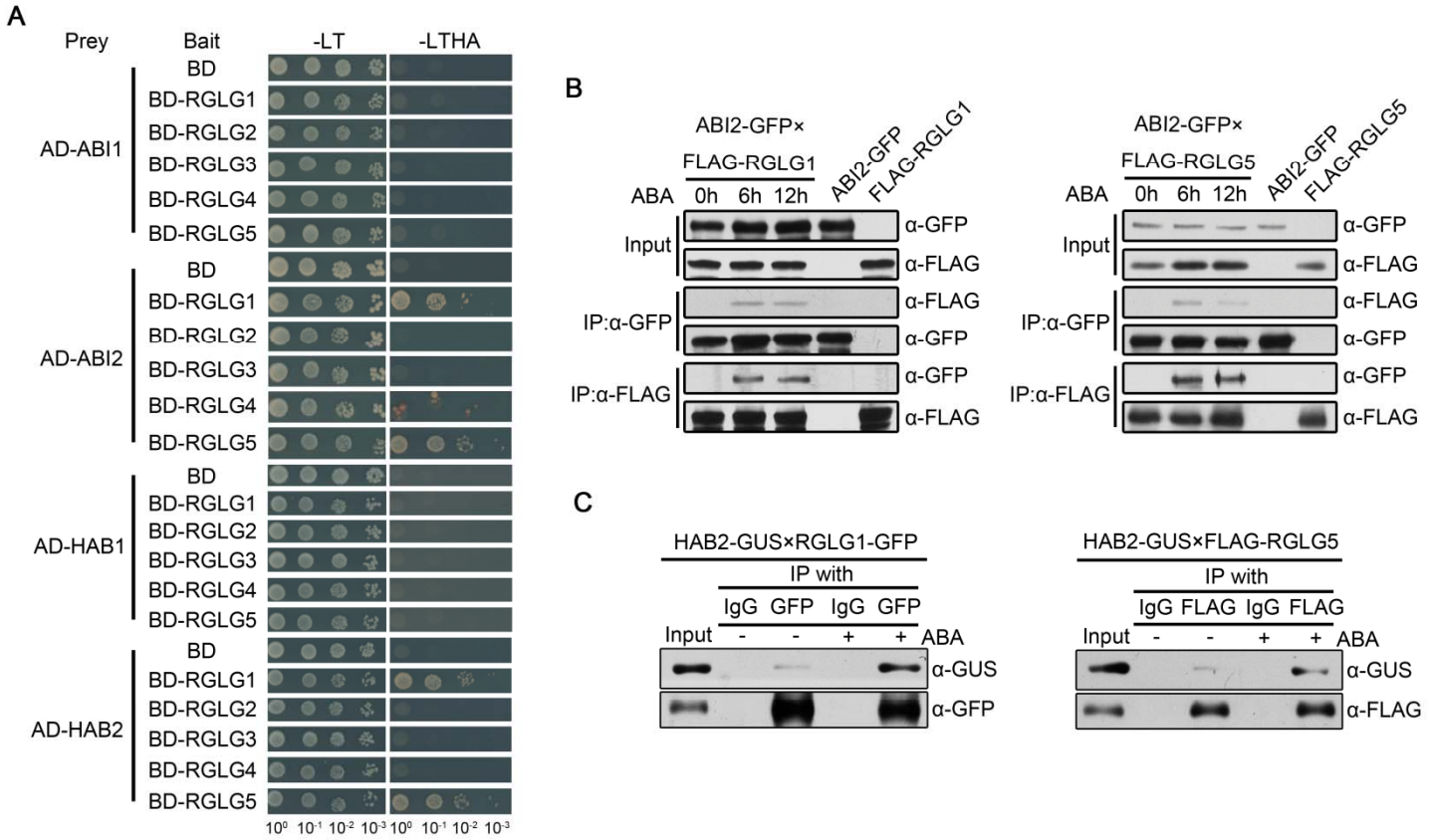

Figure 2. Interaction assays of clade A PP2Cs with RGLGs. ABI2 and HAB2 interact with RGLG1 and RGLG5 in an ABA-dependent manner.

(A) Yeast-two-hybrid analysis of interactions between PP2Cs and RGLGs. Full-length *PP2Cs* were each cloned into pGADT7Rec plasmid and used as preys; full-length *RGLGs* were inserted separately into pGBKT7 plasmid and used as baits. Each pair of prey and bait was then co-transformed into yeast. Photographs were taken 5 days after yeast cells were grown on $Leu^{-}Trp^{-}$/Yeast Nitrogen Base (YNB) and $Leu^{-}Trp^{-}His^{-}Ade^{-}$/YNB medium.

(B) ABA-enhanced interaction of ABI2 with RGLG1 and RGLG5 in *Arabidopsis*. Two-week-old transgenic *Arabidopsis* seedlings coexpressing ABI2-GFP and FLAG-RGLG1 or FLAG-RGLG5 were transferred to liquid MS medium supplemented with 50 μM ABA and sampled at the indicated time points. Immunoprecipitation was performed using anti-FLAG (IP: α-FLAG) or anti-GFP (IP: α-GFP) antibodies bounded to Protein G-Sepharose beads, separately. Anti-GFP and anti-FLAG antibodies were used to detect the proteins in total extracts (Input) and immunoprecipitates (IP).

(C) ABA-enhanced interaction of HAB2 with RGLG1 and RGLG5. HAB2-GUS and RGLG1-GFP or FLAG-RGLG5 fusions were coexpressed in *N. benthamiana* leaves by infiltration. Protein extracts were incubated with (+) or without (-) 10 μM ABA for 3 h before immunoprecipitation with anti-GFP or anti-FLAG antibodies bounded to Protein G-Sepharose beads. IgG was added in parallel as negative controls. Total extracts (Input) and immunoprecipitates (IP) were subjected to immunoblot analysis using anti-GUS, anti-GFP or anti-FLAG antibodies.

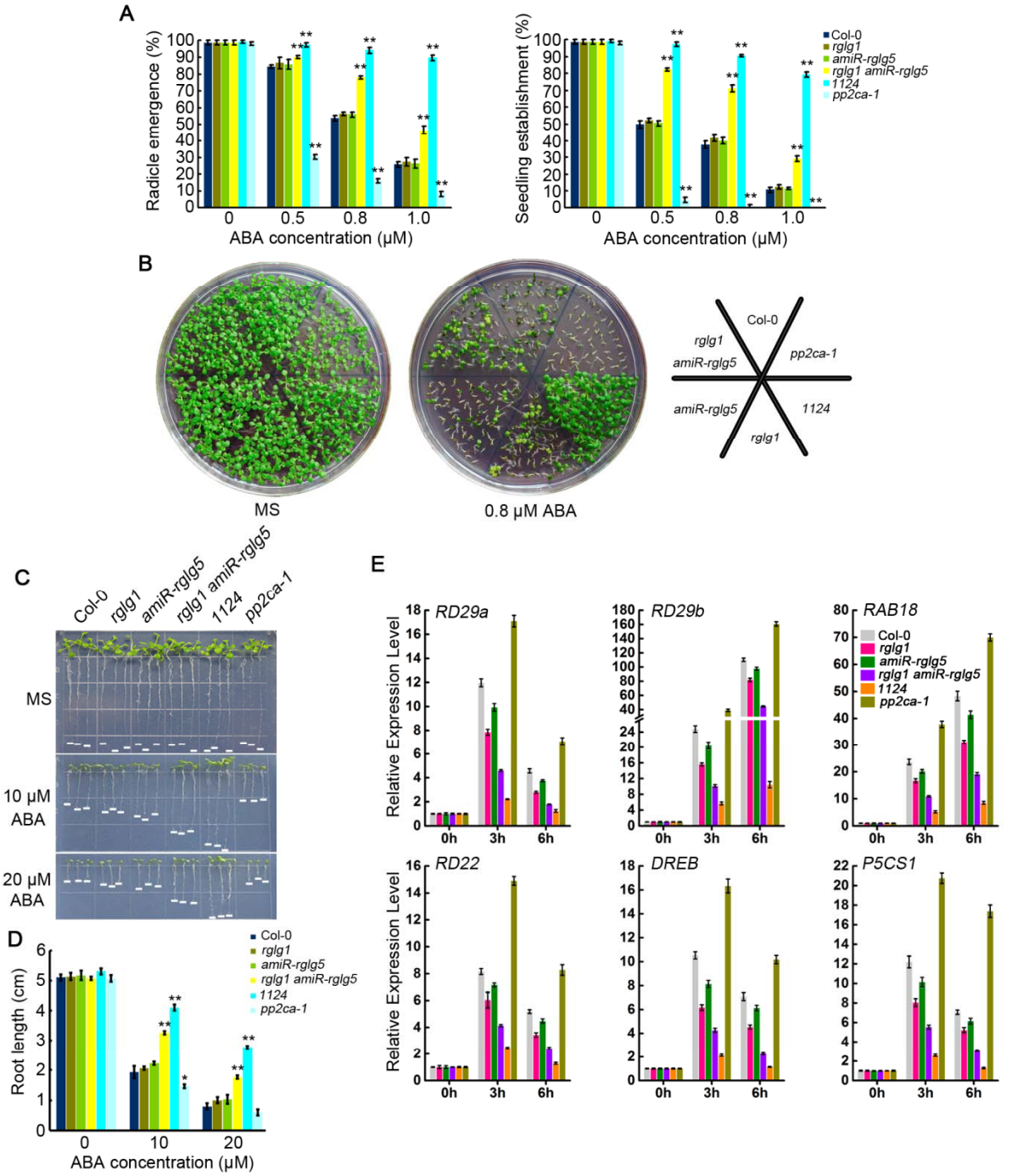

Figure 3. Diminished ABA sensitivity of the *rglg1 amiR-rglg5* double mutant.

(A) Seed germination of Col-0, *rglg1*, *rglg5*, *amiR-rglg5, rglg1 amiR-rglg5*, *pp2ca-1* and *1124.* Radicle emergence was scored after 72-h growth on MS plates containing the indicated concentrations of ABA. Seedling establishment was scored as the percentage of seeds that developed fully green expanded cotyledons after 7-day growth on MS plates containing the indicated concentrations of ABA. Bars are Mean ± standard deviation (SD) of three replications. Asterisks indicate a significant difference from wild type (Student's t-test: **, P < 0.01).

(B) Photographs of representative seedlings as in **(A)** taken 9 day after sowing on MS plates with or without 0.8 μM ABA.

(C) ABA-mediated inhibition of root growth in Col-0, *rglg1*, *rglg5*, *amiR-rglg5, rglg1 amiR-rglg5*, *pp2ca-1* and *1124*. Photos were taken 10 days after transferring 3-day-old seedlings to MS plates supplemented without or with the indicated concentrations of ABA.

(D) Primary root length quantifications of the indicated genetic backgrounds after ABA treatment indicated in **(C)**. Bars indicate Mean ± SD of thirty seedlings. Asterisks indicate a significant difference from wild type (Student's t-test: *, P < 0.05; **, P < 0.01).

(E) Expression profiles of ABA-responsive genes in Col-0, *rglg1*, *rglg5*, *amiR-rglg5, rglg1 amiR-rglg5*, *pp2ca-1* and *1124*. 7-day-old Arabidopsis seedlings were transferred to liquid MS medium containing 50 μM ABA and sampled at the indicated time points. Gene expression was examined using quantitative real-time PCR. *UBQ10* was used as the internal control, and expression levels were normalized to that measured at time 0. Data represent the mean ± SD of four technical replicas.

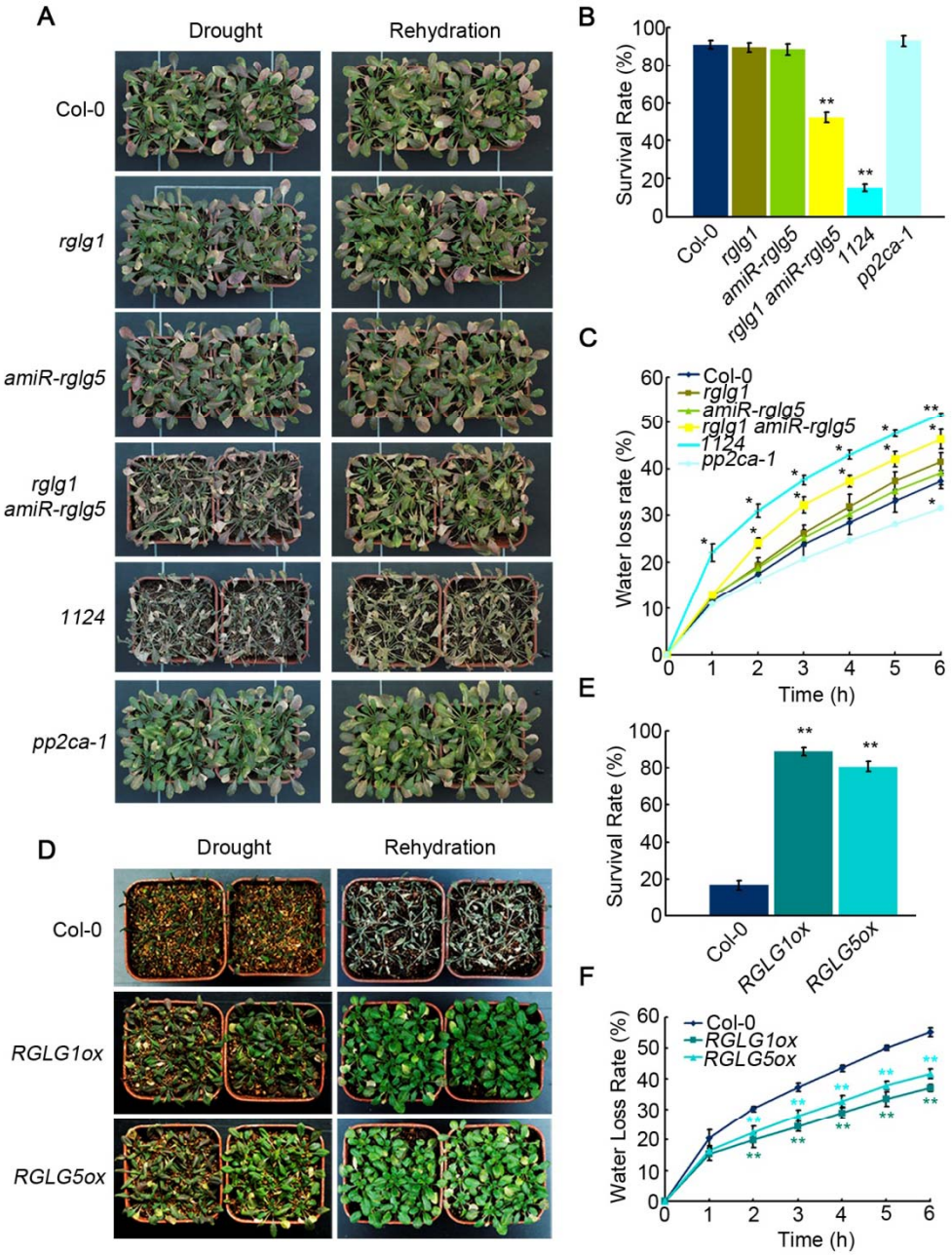

Figure 4. Enhanced water loss and drought sensitivity of *rglg1 amiR-rglg5* compared to wt or single mutants. Diminished water loss and enhanced drought resistance of overexpressing *RGLG1* or *RGLG5* plants compared to Col-0.

(A) Drought sensitivity of Col-0, *rglg1*, *amiR-rglg5, rglg1 amiR-rglg5*, *pp2ca-1* and *1124* plants. 3-week-old plants were subjected to drought stress by withholding watering (Drought) for 12 days (when the lethal effect was observed in the double mutant plants), then the plants were rewatered (Rehydration).

(B) Survival rate of plants in **(A)**. Survival rate was recorded 3 days after rehydration. Bars indicate SD calculated from three replicated experiments. Asterisks indicate significant difference from the wild type (Student's t test**,** **,P<0.01).

(C) Water loss rate of detached leaves of four-week-old plants as indicated in **(A)**. Fresh weights were monitored at the indicated time. Bars indicate SD calculated from three replications. Asterisks indicate a significant difference from wild type (Student's t-test: *, P < 0.05; **, P < 0.01).

(D) Enhanced drought tolerance of *Arabidopsis* plants overexpressing *RGLG1* or *RGLG5* compared to Col-0. 3-week-old plants were subjected to drought stress by withholding water (Drought) for 19 days (when the lethal effect was observed in the wild type plants), then the plants were rewatered (Rehydration).

(E) Percentage of plants that survived as mentioned in (**D**). Survival rate was recorded 3 days after rehydration. Bars indicate SD calculated from three independent experiments. Asterisks indicate significant difference from the wild type (Student's t test, **, P<0.01).

(F) Water loss rate of detached leaves of four-week-old *RGLG1* or *RGLG5* overexpressing plants compared to the wild type (Col-0). Fresh weight was monitored at the indicated time. Bars indicate SD calculated from three replications. Asterisks indicate a significant difference from wild type (Student's t-test: **, P < 0.01).

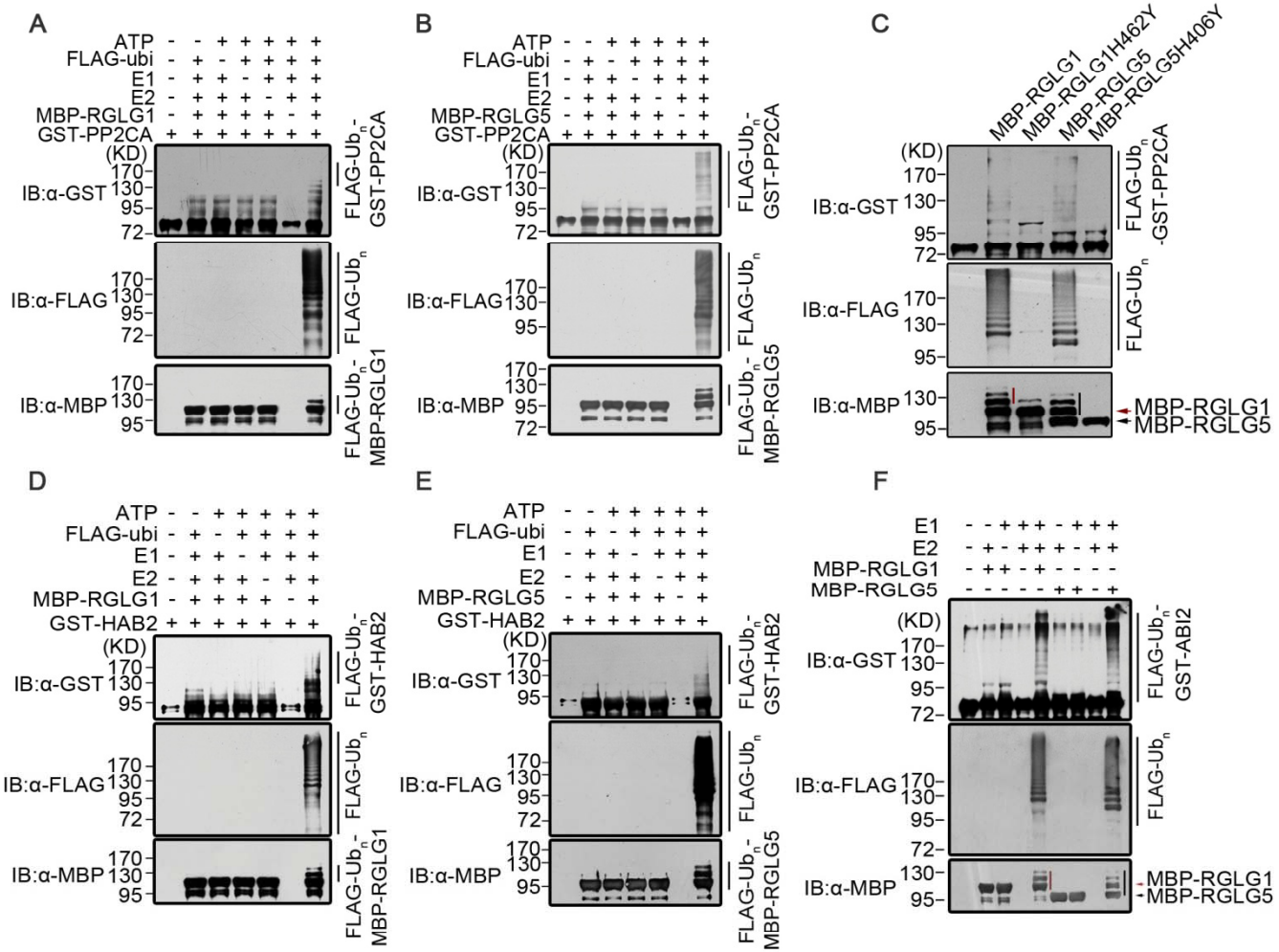

Figure 5. RGLG1- and RGLG5-mediated *in vitro* ubiquitination of PP2CA.
(A, B) *In vitro* ubiquitination of PP2CA by RGLG1 and RGLG5, respectively. Purified GST-PP2CA was incubated with ATP, FLAG-Ubiquitin, E1, E2 and MBP-RGLG1 or MBP-RGLG5 in a reaction. Each component was omitted from assays as a control. The ubiquitination products were examined by immunoblot (IB) using anti-GST, anti-FLAG and anti-MBP antibodies.
(C) *In vitro* ubiquitination of PP2CA by wt RGLG1 and RGLG5 compared to their Ring domain-mutated forms. Ubiquitinated bands were detected as in **(A)**. The first lane contains uniquely purified GST-PP2CA. Arrows indicate the position of MBP-RGLG1 (red) and MBP-RGLG5 (black). IB using anti-MBP detects self-ubiquitination of MBP-RGLG1 (red line) and MBP-RGLG5 (black line).
(D, E) *In vitro* ubiquitination of HAB2 by RGLG1and RGLG5, respectively.
(F) *In vitro* ubiquitination of ABI2 by RGLG1 and RGLG5.

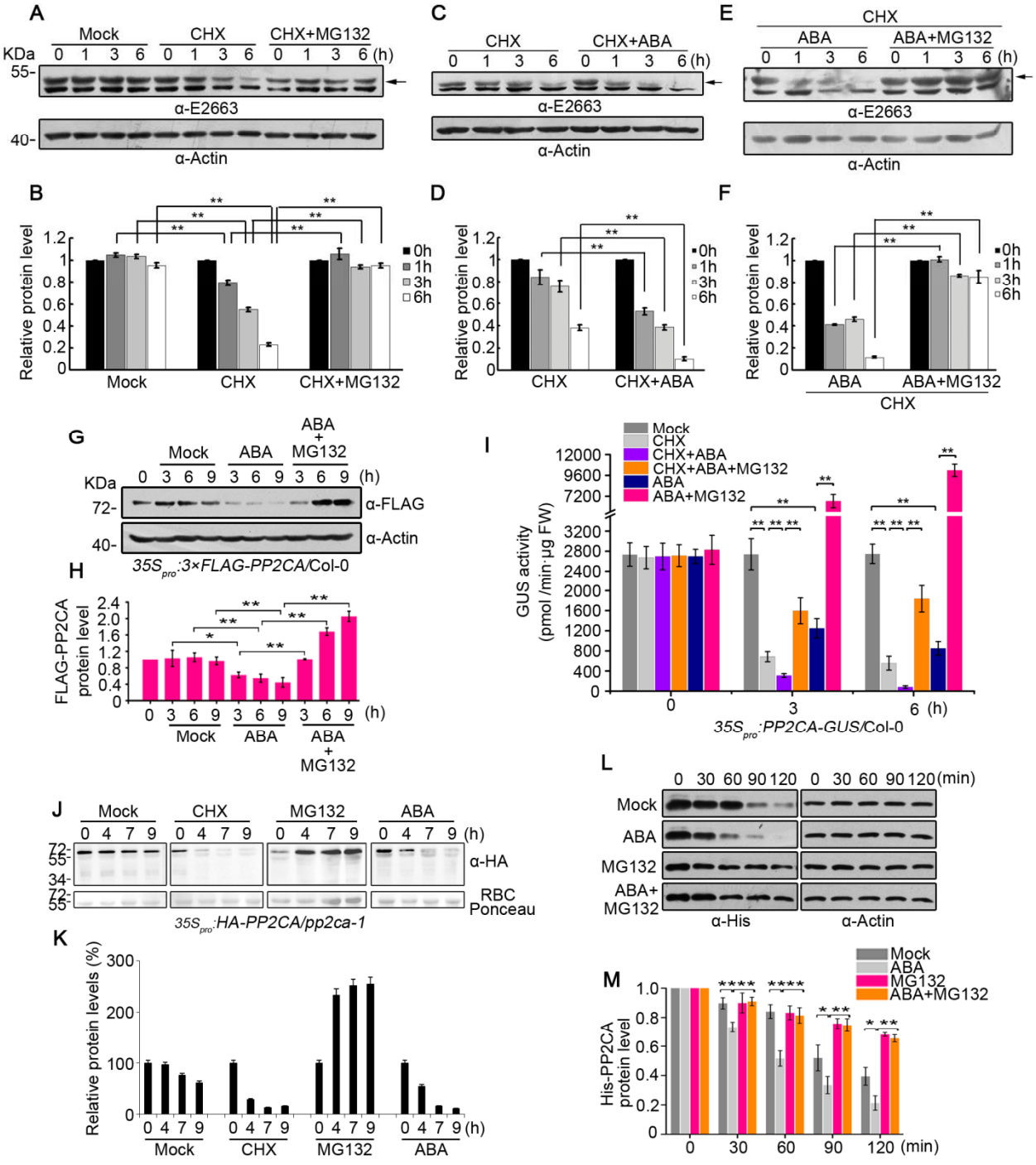
A
Mock
CHX
CHX+MG132
KDa
0 1 3 6 0 1 3 6 0 1 3 6 (h)
55-
α-E2663
40-
α-Actin
B
Relative protein level
Mock
CHX
CHX+MG132
0h
1h
3h
6h
C
CHX
CHX+ABA
α-E2663
α-Actin
D
E
CHX
ABA
ABA+MG132
α-E2663
α-Actin
F
ABA
ABA+MG132
CHX
G
ABA
+
MG132
Mock
ABA
0 3 6 9 3 6 9 3 6 9 (h)
72-
α-FLAG
40-
α-Actin
35S pro:3×FLAG-PP2CA/Col-0
H
FLAG-PP2CA protein level
I
Mock
CHX
CHX+ABA
CHX+ABA+MG132
ABA
ABA+MG132
GUS activity (pmol /min·μg FW)
35S pro:PP2CA-GUS/Col-0
J
Mock
CHX
MG132
ABA
0 4 7 9 (h)
72-
55-
34-
α-HA
RBC Ponceau
35S pro:HA-PP2CA/pp2ca-1
K
Relative protein levels (%)
L
0 30 60 90 120 0 30 60 90 120 (min)
Mock
ABA
MG132
ABA+ MG132
α-His
α-Actin
M
His-PP2CA protein level
Mock
ABA
MG132
ABA+MG132
0 30 60 90 120 (min)

Figure 6. ABA enhances PP2CA degradation mediated by the 26S proteasome pathway.
(A) PP2CA is degraded by the 26S proteasome. Two-week-old etiolated seedlings were transferred to liquid MS medium and were mock-, 100 μM CHX- or 100 μM CHX+50 μM MG132-treated for the indicated time period. Total protein extracts were prepared for western blot analysis. The α-E2663 polyclonal antibody of PP2CA was used to determine the endogenous PP2CA protein level (arrow). Actin was used as a loading control. The relative protein levels of PP2CA at 0 h were set as 1. Bars indicate the mean ± SD from the three replicas. Asterisks indicate a significant difference between the indicated comparisons (Student's t-test: **, $P < 0.01$).
(B) Quantification of signal intensity in **(A)** by Image J software.
(C) ABA enhances PP2CA degradation. Two-week-old etiolated seedlings were treated with 100 μM CHX or 100 μM CHX+50 μM ABA for the indicated time period.
(D) Quantification of signal intensity in **(C)** by Image J software .
(E) ABA enhances PP2CA degradation through the 26S proteasome. Two-week-old etiolated seedlings of Col-0 were treated with 100 μM CHX+50 μM ABA or 100 μM CHX+50 μM ABA+50 μM MG132 for the indicated time period.
(F) Quantification of signal intensity in **(E)** by Image J software.
(G) PP2CA protein dynamics after different treatments determined by Western blot analysis. Two-week-old seedlings constitutively overexpressing 3×FLAG-PP2CA were transferred to liquid MS medium and were mock-, 50 μM ABA- or 50 μM ABA+50 μM MG132-treated, and sampled at the indicated time points. Western blot was performed using anti-FLAG antibody. Actin was analyzed as a loading control.
(H) Three-independent experiments as in **(G)** were performed and the signal intensity was determined by Image J software. The protein levels of FLAG-PP2CA without treatment (0 h) were defined as "1". Bars indicate the mean ± SD from the three replicas. Student's t tests were used to determine significant levels of the indicated comparisons. *, $P < 0.05$; **, $P < 0.01$.
(I) Quantified GUS activities in protein extracts prepared from plants expressing PP2CA-GUS submitted to different treatments. Seven-day-old seedlings were mock-treated or treated with 50 μM ABA, 50 μM MG132, 100 μM cycloheximide (CHX) or the indicated combinations. Samples were harvested at the indicated time points for measuring GUS activity. Bars indicate the mean ± SD from the three replicas. Student's t tests were used to determine significant levels of the indicated comparisons. *, $P < 0.05$; **, $P < 0.01$.
(J) Effect of CHX, MG132 and ABA treatment on HA-PP2CA protein levels in *pp2ca-1* background. 10-d-old seedlings expressing HA-tagged PP2CA were either mock- or chemically-treated with 100 μM CHX, 50 μM MG132 or 50 μM ABA for the indicated time period. Immunoblot analysis using anti-HA was performed to quantify protein levels.
(K) Three-independent experiments as in **(J)** were performed and the histogram represents the average relative protein level with respect to time 0 (error bars indicate standard error).
(L) In vitro degradation of His-PP2CA. Whole cell extracts prepared from 7-day-old seedlings of Col-0 were incubated with purified His-PP2CA at 15ºC supplemented with or without different combinations of ABA and MG132, and sampled at the indicated time points. Anti-His antibody was used to detect protein dynamics and actin was analyzed as a loading control.
(M) Three-independent experiments as in **(L)** were performed and the signal intensity was determined by Image J software. The protein levels of His-PP2CA in Col-0 extracts with indicated treatments at 0 min were defined as "1". Bars indicate the mean ± SD from the three replicas. Student's t tests were used to determine significant levels of the indicated comparisons. *, $P < 0.05$; **, $P < 0.01$.

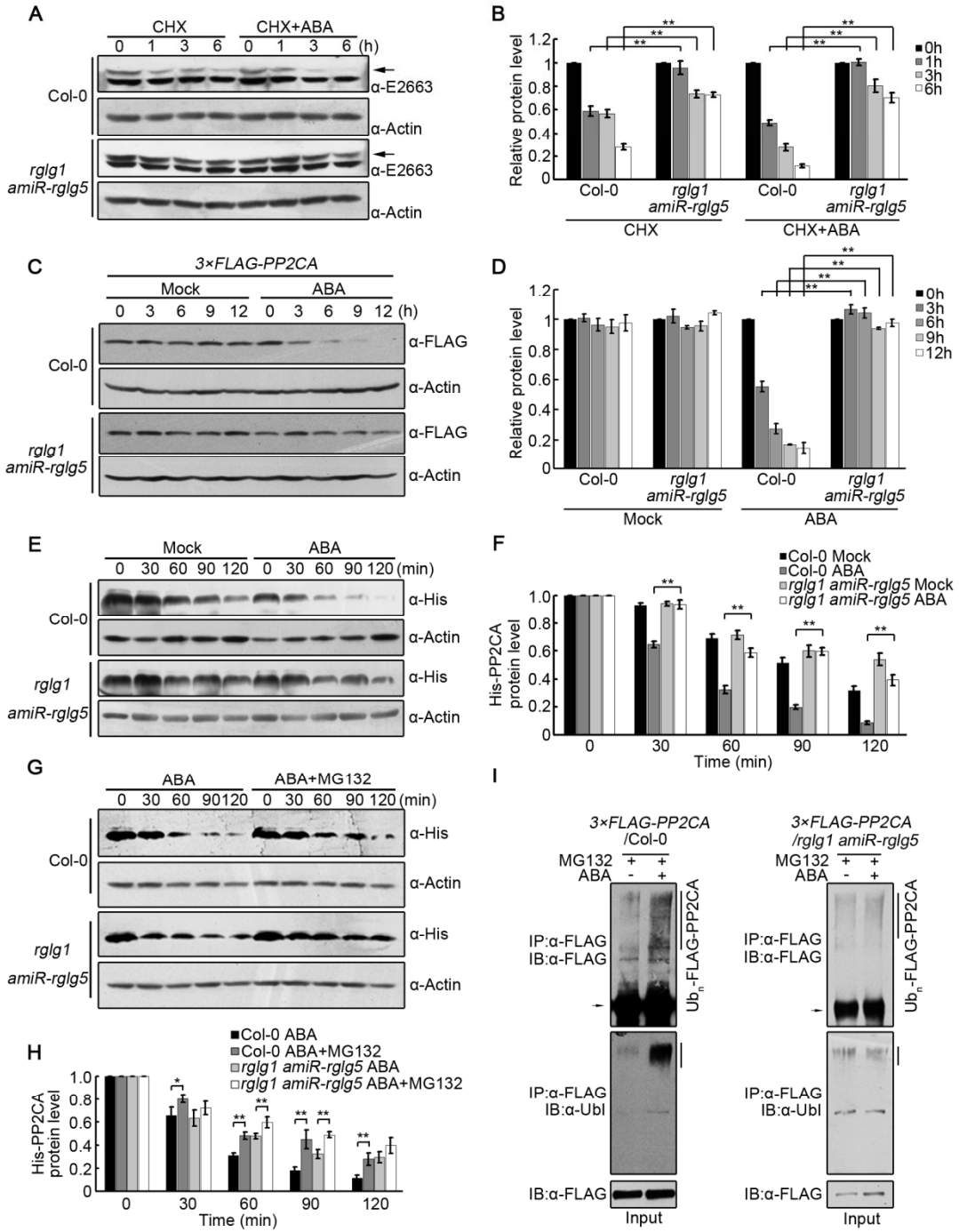

Figure 7. RGLG1- and RGLG5-mediated protein turnover of PP2CA.
(A) PP2CA protein levels in Col-0 versus *rglg1 amiR-rglg5* in response to ABA. Two-week-old etiolated seedlings of Col-0 and *rglg1 amiR-rglg5* were treated with 100 μM CHX or 100 μM CHX+50 μM ABA for 0, 1, 3, 6 h. Samples were harvested for Western blot analysis using α-E2663 to detect endogenous PP2CA protein levels (arrow) in Col-0 and *rglg1 amiR-rglg5*. Actin was analyzed as a loading control.
(B) The signal intensity in **(A)** was determined by Image J software.
(C) ABA enhances PP2CA protein degradation. Two-week-old seedlings of transgenic *Arabidopsis* constitutively expressing 3×FLAG-PP2CA in Col-0 or *rglg1 amiR-rglg5* backgrounds were transferred to liquid MS medium without (Mock) or with 50 μM ABA for the indicated time period. Anti-FLAG was used to detect FLAG-PP2CA. Actin was analyzed as a loading control.
(D) The signal intensity in **(C)** was determined by Image J software. The relative protein levels of FLAG-PP2CA at time point 0 h were set as"1". Bars indicate the mean ± SD from the three replicas. Student's t tests were used to determine significant levels of the indicated comparisons. **, $P < 0.01$.
(E, G) *In vitro* degradation of His-PP2CA by protein extracts prepared from 7-day-old Col-0 or *rglg1 amiR-rglg5* seedlings. Purified His-PP2CA was incubated for the indicated time period in the absence (Mock) or presence of ABA **(E)** or in presence of ABA or ABA+MG132 **(G)**. Protein dynamics of PP2CA was analyzed by Western blot using anti-His antibody. Actin was analyzed as a loading control.
(F, H) The signal intensity was determined by Image J software from three-independent experiments as in **(E)** and **(G)**, respectively. The relative protein levels of His-PP2CA in Col-0 and *rglg1 amiR-rglg5* at time point 0 min were defined as "1". Bars indicate the mean ± SD from three replicas. Student's t tests were used to determine significance of the indicated comparisons. **, $P < 0.01$.
(I) *In vivo* ubiquitination of PP2CA in different genetic backgrounds. FLAG-PP2CA protein was immunoprecipated from 2-week-old *35S::3×FLAG-PP2CA*/Col-0 and *35S::3×FLAG-PP2CA*/*rglg1 amiR-rglg5* seedlings treated with MG132 or ABA+MG132. Immunoprecipated proteins were detected by immunoblotting using anti-FLAG and anti-ubiquitin antibodies, respectively.

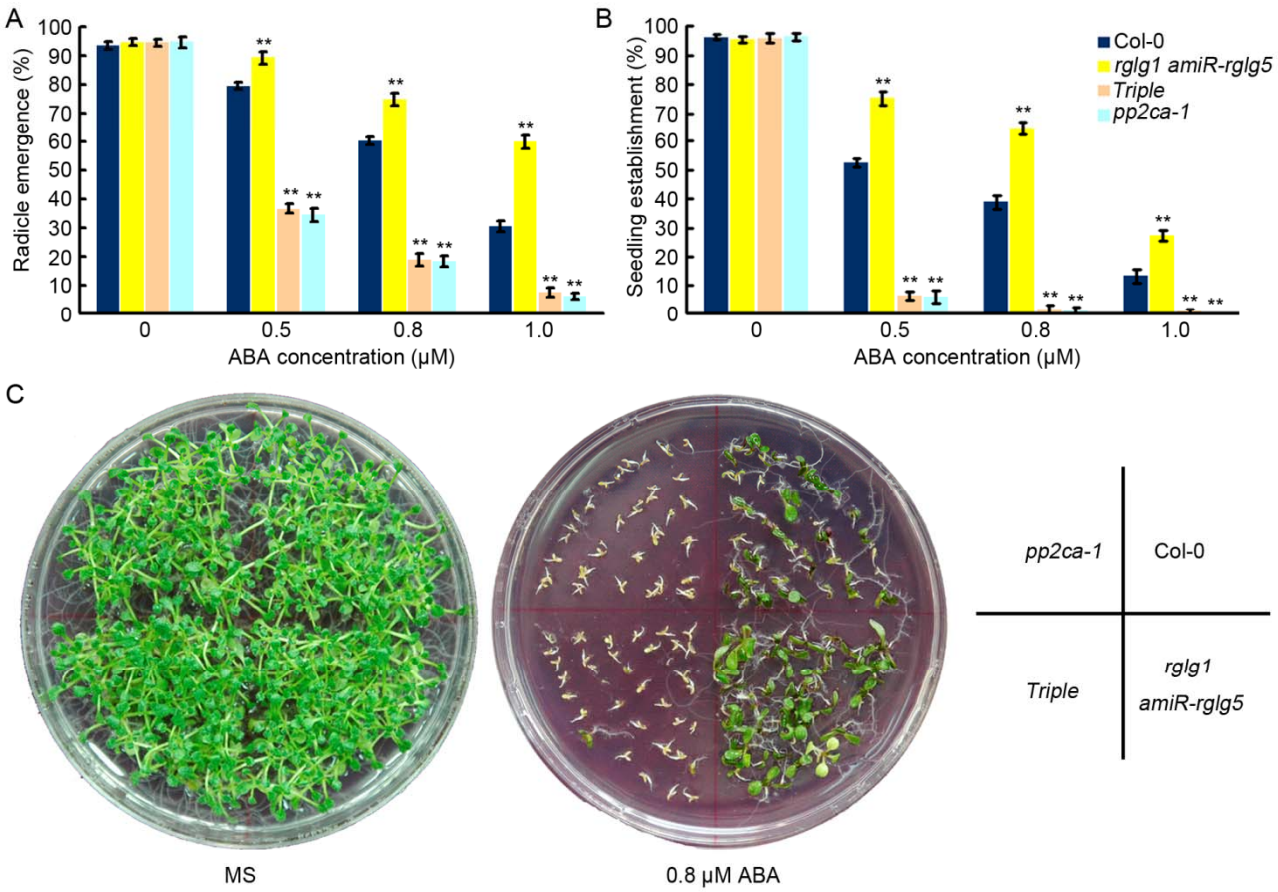

Figure 8. ABA insensitivity of *rglg1 amiR-rglg5* is dependent on PP2CA activity.
(A) Seed germination and **(B)** Seeedling establishment of Col-0, *rglg1 amiR-rglg5* double, *rglg1 amiR-rglg5 pp2ca-1* triple and *pp2ca-1* mutants. Radicle emergence was scored after 72-h growth on MS plates containing the indicated concentrations of ABA **(A)**. Seedling establishment was scored as the percentage of seeds that developed fully green expanded cotyledons after 7-day growth on MS plates containing the indicated concentrations of ABA **(B)**. Bars are Mean ± SD of three replicas. Asterisks indicate a significant difference from wild type (Student's t-test: **, P < 0.01).
(C) Photographs of representative plates were taken 12 day after sowing the indicated genetic backgrounds on MS plates lacking or containing 0.8 μM ABA.

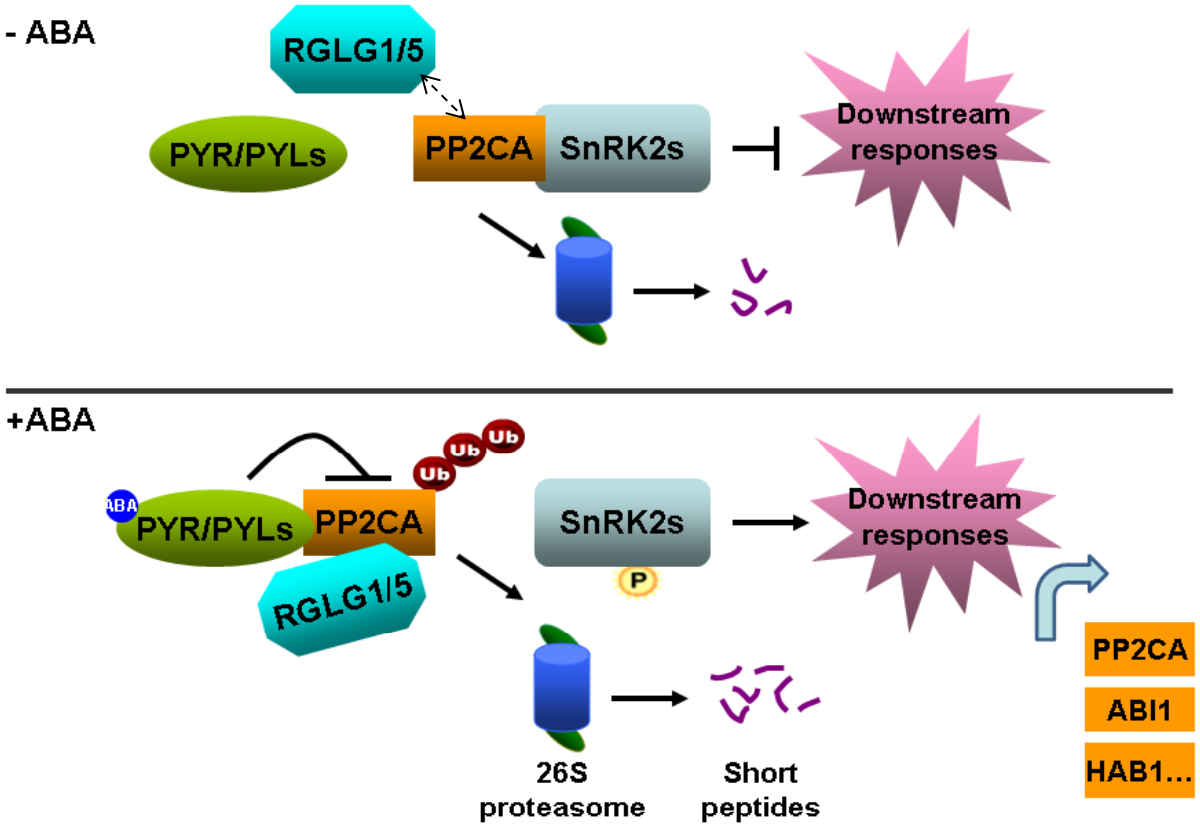

Figure 9. Proposed model for the enhanced degradation of PP2CA via the 26S proteasome mediated by ABA and RGLG1/5. Under non-stress conditions (-ABA, low ABA levels), RGLG1 and RGLG5 show less interaction with PP2CA (discontinous arrow) or there is less PP2CA available for interaction because *PP2CA* transcripts are up-regulated by ABA. PP2CA interacts with SnRK2s, which prevents their activation and leads to inhibition of downstream ABA responses. PP2CA levels under non-stress conditions are regulated by RGLG1/5 or additional unidentified E3s. When plants are challenged (+ABA, high ABA levels), ABA promotes the interaction of PYR/PYLs with PP2CA, inhibiting its phosphatase activity. ABA facilitates RGLG1/5 interaction with PP2CA, which leads to its ubiquitination and degradation via the 26S proteasome pathway, resulting in full activation of ABA signaling. As a negative feedback mechanism, ABA also increases *PP2CA* and clade A *PP2C* transcripts.

Parsed Citations

Abe, H., Urao, T., Ito, T., Seki, M., Shinozaki, K., and Yamaguchi-Shinozaki, K. (2003). Arabidopsis AtMYC2 (bHLH) and AtMYB2 (MYB) function as transcriptional activators in abscisic acid signaling. Plant Cell 15, 63-78.
Pubmed: Author and Title
CrossRef: Author and Title
Google Scholar: Author Only Title Only Author and Title

Antoni, R., Gonzalez-Guzman, M., Rodriguez, L., Rodrigues, A., Pizzio, G.A., and Rodriguez, P.L. (2012). Selective inhibition of clade A phosphatases type 2C by PYR/PYL/RCAR abscisic acid receptors. Plant Physiol. 158, 970-980.
Pubmed: Author and Title
CrossRef: Author and Title
Google Scholar: Author Only Title Only Author and Title

Antoni, R., Gonzalez-Guzman, M., Rodriguez, L., Peirats-Llobet, M., Pizzio, G.A., Fernandez, M.A., De Winne, N., De Jaeger, G., Dietrich, D., Bennett, M.J., and Rodriguez, P.L. (2013). PYRABACTIN RESISTANCE1-LIKE8 plays an important role for the regulation of abscisic acid signaling in root. Plant Physiol. 161, 931-941.
Pubmed: Author and Title
CrossRef: Author and Title
Google Scholar: Author Only Title Only Author and Title

Brandt,B., Munemasa,S., Wang,C., Nguyen,D., Yong,T., Yang,P.G., Poretsky,E., Belknap,T.F., Waadt,R., Aleman,F. and Schroeder,J.I. (2015). Calcium specificity signaling mechanisms in abscisic acid signal transduction in Arabidopsis guard cells. Elife. 4,e03599
Pubmed: Author and Title
CrossRef: Author and Title
Google Scholar: Author Only Title Only Author and Title

Bueso, E., Rodriguez, L., Lorenzo-Orts, L., Gonzalez-Guzman, M., Sayas, E., Munoz-Bertomeu, J., Ibanez, C., Serrano, R., and Rodriguez, P.L. (2014). The single-subunit RING-type E3 ubiquitin ligase RSL1 targets PYL4 and PYR1 ABA receptors in plasma membrane to modulate abscisic acid signaling. Plant J. 80, 1057-1071.
Pubmed: Author and Title
CrossRef: Author and Title
Google Scholar: Author Only Title Only Author and Title

Cai, Z., Liu, J., Wang, H., Yang, C., Chen, Y., Li, Y., Pan, S., Dong, R., Tang, G., Barajas-Lopez Jde, D., Fujii, H., and Wang, X. (2014). GSK3-like kinases positively modulate abscisic acid signaling through phosphorylating subgroup III SnRK2s in Arabidopsis. Proc. Natl. Acad. Sci. USA 111, 9651-9656.
Pubmed: Author and Title
CrossRef: Author and Title
Google Scholar: Author Only Title Only Author and Title

Clough, S.J., and Bent, A.F. (1998). Floral dip: a simplified method for Agrobacterium-mediated transformation of Arabidopsis thaliana. Plant J. 16, 735-743.
Pubmed: Author and Title
CrossRef: Author and Title
Google Scholar: Author Only Title Only Author and Title

Curtis, M.D., and Grossniklaus, U. (2003). A gateway cloning vector set for high-throughput functional analysis of genes in planta. Plant Physiol. 133, 462-469.
Pubmed: Author and Title
CrossRef: Author and Title
Google Scholar: Author Only Title Only Author and Title

Cutler, S.R., Rodriguez, P.L., Finkelstein, R.R., and Abrams, S.R. (2010). Abscisic acid: emergence of a core signaling network. Annu. Rev. Plant Biol. 61, 651-679.
Pubmed: Author and Title
CrossRef: Author and Title
Google Scholar: Author Only Title Only Author and Title

Deblaere, R., Bytebier, B., De Greve, H., Deboeck, F., Schell, J., Van Montagu, M., and Leemans, J. (1985). Efficient octopine Ti plasmid-derived vectors for Agrobacterium-mediated gene transfer to plants. Nucleic Acids Res. 13, 4777-4788.
Pubmed: Author and Title
CrossRef: Author and Title
Google Scholar: Author Only Title Only Author and Title

Deshaies, R.J., and Joazeiro, C.A. (2009). RING domain E3 ubiquitin ligases. Annu. Rev. Biochem. 78, 399-434.
Pubmed: Author and Title
CrossRef: Author and Title
Google Scholar: Author Only Title Only Author and Title

Finkelstein, R. (2013). Abscisic Acid synthesis and response. Arabidopsis Book 11, e0166.
Pubmed: Author and Title
CrossRef: Author and Title
Google Scholar: Author Only Title Only Author and Title

Fujii, H., and Zhu, J.K. (2009). Arabidopsis mutant deficient in 3 abscisic acid-activated protein kinases reveals critical roles in growth, reproduction, and stress. Proc. Natl. Acad. Sci. USA 106, 8380-8385.
Pubmed: Author and Title

CrossRef: Author and Title
Google Scholar: Author Only Title Only Author and Title

Fujii, H., Chinnusamy, V., Rodrigues, A., Rubio, S., Antoni, R., Park, S.Y., Cutler, S.R., Sheen, J., Rodriguez, P.L., and Zhu, J.K. (2009). In vitro reconstitution of an abscisic acid signalling pathway. Nature 462, 660-664.
Pubmed: Author and Title
CrossRef: Author and Title
Google Scholar: Author Only Title Only Author and Title

Fujita,Y., Nakashima,K., Yoshida,T., Katagiri,T., Kidokoro,S., Kanamori,N., Umezawa,T., Fujita,M., Maruyama,K., Ishiyama,K., Kobayashi,M., Nakasone,S., Yamada,K., Ito,T., Shinozaki,K. and Yamaguchi-Shinozaki,K. (2009). Three SnRK2 protein kinases are the main positive regulators of abscisic acid signaling in response to water stress in Arabidopsis. Plant Cell Physiol 50, 2123-2132.
Pubmed: Author and Title
CrossRef: Author and Title
Google Scholar: Author Only Title Only Author and Title

Geiger, D., Scherzer, S., Mumm, P., Stange, A., Marten, I., Bauer, H., Ache, P., Matschi, S., Liese, A., Al-Rasheid, K.A., Romeis, T., and Hedrich, R. (2009). Activity of guard cell anion channel SLAC1 is controlled by drought-stress signaling kinase-phosphatase pair. Proc. Natl. Acad. Sci. USA 106, 21425-21430.
Pubmed: Author and Title
CrossRef: Author and Title
Google Scholar: Author Only Title Only Author and Title

Gonzalez-Guzman, M., Pizzio, G.A., Antoni, R., Vera-Sirera, F., Merilo, E., Bassel, G.W., Fernandez, M.A., Holdsworth, M.J., Perez-Amador, M.A., Kollist, H., and Rodriguez, P.L. (2012). Arabidopsis PYR/PYL/RCAR receptors play a major role in quantitative regulation of stomatal aperture and transcriptional response to abscisic acid. Plant Cell 24, 2483-2496.
Pubmed: Author and Title
CrossRef: Author and Title
Google Scholar: Author Only Title Only Author and Title

Hubbard, K.E., Nishimura, N., Hitomi, K., Getzoff, E.D., and Schroeder, J.I. (2010). Early abscisic acid signal transduction mechanisms: newly discovered components and newly emerging questions. Genes Dev. 24, 1695-1708.
Pubmed: Author and Title
CrossRef: Author and Title
Google Scholar: Author Only Title Only Author and Title

Irigoyen, M.L., Iniesto, E., Rodriguez, L., Puga, M.I., Yanagawa, Y., Pick, E., Strickland, E., Paz-Ares, J., Wei, N., De Jaeger, G., Rodriguez, P.L., Deng, X.W., and Rubio, V. (2014). Targeted degradation of abscisic acid receptors is mediated by the ubiquitin ligase substrate adaptor DDA1 in Arabidopsis. Plant Cell 26, 712-728.
Pubmed: Author and Title
CrossRef: Author and Title
Google Scholar: Author Only Title Only Author and Title

Kelley, D.R., and Estelle, M. (2012). Ubiquitin-mediated control of plant hormone signaling. Plant Physiol. 160, 47-55.
Pubmed: Author and Title
CrossRef: Author and Title
Google Scholar: Author Only Title Only Author and Title

Kobayashi, Y., Murata, M., Minami, H., Yamamoto, S., Kagaya, Y., Hobo, T., Yamamoto, A., and Hattori, T. (2005). Abscisic acid-activated SNRK2 protein kinases function in the gene-regulation pathway of ABA signal transduction by phosphorylating ABA response element-binding factors. Plant J. 44, 939-949.
Pubmed: Author and Title
CrossRef: Author and Title
Google Scholar: Author Only Title Only Author and Title

Kong, L.Y., Cheng, J.K., Zhu, Y.J., Ding, Y.L., Meng, J.J., Chen, Z.Z., Xie, Q., Guo, Y., Li, J.G., Yang, S.H., and Gong, Z.Z. (2015). Degradation of the ABA co-receptor ABI1 by PUB12/13 U-box E3 ligases. Nature Communications 6.
Pubmed: Author and Title
CrossRef: Author and Title
Google Scholar: Author Only Title Only Author and Title

Kuhn, J.M., Boisson-Dernier, A., Dizon, M.B., Maktabi, M.H., and Schroeder, J.I. (2006). The protein phosphatase AtPP2CA negatively regulates abscisic acid signal transduction in Arabidopsis, and effects of abh1 on AtPP2CA mRNA. Plant Physiol. 140, 127-139.
Pubmed: Author and Title
CrossRef: Author and Title
Google Scholar: Author Only Title Only Author and Title

Lang, V., and Palva, E.T. (1992). The expression of a rab-related gene, rab18, is induced by abscisic acid during the cold acclimation process of Arabidopsis thaliana (L.) Heynh. Plant Mol. Biol. 20, 951-962.
Pubmed: Author and Title
CrossRef: Author and Title
Google Scholar: Author Only Title Only Author and Title

Lee, S.C., Lan, W., Buchanan, B.B., and Luan, S. (2009). A protein kinase-phosphatase pair interacts with an ion channel to regulate ABA signaling in plant guard cells. Proc. Natl. Acad. Sci. USA 106, 21419-21424.
Pubmed: Author and Title
CrossRef: Author and Title
Google Scholar: Author Only Title Only Author and Title

Liu, H., and Stone, S.L. (2010). Abscisic acid increases Arabidopsis ABI5 transcription factor levels by promoting KEG E3 ligase self-ubiquitination and proteasomal degradation. Plant Cell 22, 2630-2641.
Pubmed: Author and Title
CrossRef: Author and Title
Google Scholar: Author Only Title Only Author and Title

Liu, H., and Stone, S.L. (2011). E3 ubiquitin ligases and abscisic acid signaling. Plant Signal. Behav. 6, 344-348.
Pubmed: Author and Title
CrossRef: Author and Title
Google Scholar: Author Only Title Only Author and Title

Ma, Y., Szostkiewicz, I., Korte, A., Moes, D., Yang, Y., Christmann, A., and Grill, E. (2009). Regulators of PP2C phosphatase activity function as abscisic acid sensors. Science 324, 1064-1068.
Pubmed: Author and Title
CrossRef: Author and Title
Google Scholar: Author Only Title Only Author and Title

Nakashima,K., Fujita,Y., Kanamori,N., Katagiri,T., Umezawa,T., Kidokoro,S., Maruyama,K., Yoshida,T., Ishiyama,K., Kobayashi,M., Shinozaki,K. and Yamaguchi-Shinozaki,K. (2009). Three Arabidopsis SnRK2 protein kinases, SRK2D/SnRK2.2, SRK2E/SnRK2.6/OST1 and SRK2I/SnRK2.3, involved in ABA signaling are essential for the control of seed development and dormancy. Plant Cell Physiol 50, 1345-1363.
Pubmed: Author and Title
CrossRef: Author and Title
Google Scholar: Author Only Title Only Author and Title

Nishimura,N., Sarkeshik,A., Nito,K., Park,S.Y., Wang,A., Carvalho,P.C., Lee,S., Caddell,D.F., Cutler,S.R., Chory,J., Yates,J.R. and Schroeder,J.I. (2010). PYR/PYL/RCAR family members are major in-vivo ABI1 protein phosphatase 2C-interacting proteins in Arabidopsis. Plant J. 61, 290-299.
Pubmed: Author and Title
CrossRef: Author and Title
Google Scholar: Author Only Title Only Author and Title

Nordin,K., Vahala,T. and Palva,E.T. (1993). Differential expression of two related, low-temperature-induced genes in Arabidopsis thaliana (L.) Heynh. Plant Mol. Biol. 21, 641-653.
Pubmed: Author and Title
CrossRef: Author and Title
Google Scholar: Author Only Title Only Author and Title

Park,S.Y., Fung,P., Nishimura,N., Jensen,D.R., Fujii,H., Zhao,Y., Lumba,S., Santiago,J., Rodrigues,A., Chow,T.F.F., Alfred,S.E., Bonetta,D., Finkelstein,R., Provart,N.J., Desveaux,D., Rodriguez,P.L., McCourt,P., Zhu,J.K., Schroeder,J.I., Volkman,B.F. and Cutler,S.R. (2009). Abscisic Acid Inhibits Type 2C Protein Phosphatases via the PYR/PYL Family of START Proteins. Science 324, 1068-1071.
Pubmed: Author and Title
CrossRef: Author and Title
Google Scholar: Author Only Title Only Author and Title

Pizzio,G.A., Rodriguez,L., Antoni,R., Gonzalez-Guzman,M., Yunta,C., Merilo,E., Kollist,H., Albert,A. and Rodriguez,P.L. (2013). The PYL4 A194T mutant uncovers a key role of PYR1-LIKE4/PROTEIN PHOSPHATASE 2CA interaction for abscisic acid signaling and plant drought resistance. Plant Physiol 163, 441-455.
Pubmed: Author and Title
CrossRef: Author and Title
Google Scholar: Author Only Title Only Author and Title

Rubio,S., Rodrigues,A., Saez,A., Dizon,M.B., Galle,A., Kim,T.H., Santiago,J., Flexas,J., Schroeder,J.I. and Rodriguez,P.L. (2009). Triple loss of function of protein phosphatases type 2C leads to partial constitutive response to endogenous abscisic acid. Plant Physiol 150, 1345-1355.
Pubmed: Author and Title
CrossRef: Author and Title
Google Scholar: Author Only Title Only Author and Title

Santiago,J., Rodrigues,A., Saez,A., Rubio,S., Antoni,R., Dupeux,F., Park,S.Y., Marquez,J.A., Cutler,S.R. and Rodriguez,P.L. (2009). Modulation of drought resistance by the abscisic acid receptor PYL5 through inhibition of clade A PP2Cs. Plant J. 60, 575-588.
Pubmed: Author and Title
CrossRef: Author and Title
Google Scholar: Author Only Title Only Author and Title

Santner,A. and Estelle,M. (2009). Recent advances and emerging trends in plant hormone signalling. Nature 459, 1071-1078.
Pubmed: Author and Title
CrossRef: Author and Title
Google Scholar: Author Only Title Only Author and Title

Sheen,J. (1998). Mutational analysis of protein phosphatase 2C involved in abscisic acid signal transduction in higher plants. Proc. Natl. Acad. Sci. U. S. A 95, 975-980.
Pubmed: Author and Title
CrossRef: Author and Title
Google Scholar: Author Only Title Only Author and Title

Strizhov,N., Abraham,E., Okresz,L., Blickling,S., Zilberstein,A., Schell,J., Koncz,C. and Szabados,L. (1997). Differential expression of two P5CS genes controlling proline accumulation during salt-stress requires ABA and is regulated by ABA1, ABI1 and AXR2 in Arabidopsis. Plant J. 12, 557-569.

Pubmed: Author and Title
CrossRef: Author and Title
Google Scholar: Author Only Title Only Author and Title

Szostkiewicz,I., Richter,K., Kepka,M., Demmel,S., Ma,Y., Korte,A., Assaad,F.F., Christmann,A. and Grill,E. (2010). Closely related receptor complexes differ in their ABA selectivity and sensitivity. Plant J. 61, 25-35.
Pubmed: Author and Title
CrossRef: Author and Title
Google Scholar: Author Only Title Only Author and Title

Umezawa,T., Sugiyama,N., Mizoguchi,M., Hayashi,S., Myouga,F., Yamaguchi-Shinozaki,K., Ishihama,Y., Hirayama,T. and Shinozaki,K. (2009). Type 2C protein phosphatases directly regulate abscisic acid-activated protein kinases in Arabidopsis. Proc. Natl. Acad. Sci. U. S. A 106, 17588-17593.
Pubmed: Author and Title
CrossRef: Author and Title
Google Scholar: Author Only Title Only Author and Title

Umezawa,T., Sugiyama,N., Takahashi,F., Anderson,J.C., Ishihama,Y., Peck,S.C. and Shinozaki,K. (2013). Genetics and phosphoproteomics reveal a protein phosphorylation network in the abscisic acid signaling pathway in Arabidopsis thaliana. Sci. Signal. 6, rs8.
Pubmed: Author and Title
CrossRef: Author and Title
Google Scholar: Author Only Title Only Author and Title

Vilela,B., Najar,E., Lumbreras,V., Leung,J. and Pages,M. (2015). Casein Kinase 2 Negatively Regulates Abscisic Acid-Activated SnRK2s in the Core Abscisic Acid-Signaling Module. Mol. Plant 8, 709-721.
Pubmed: Author and Title
CrossRef: Author and Title
Google Scholar: Author Only Title Only Author and Title

Vlad,F., Rubio,S., Rodrigues,A., Sirichandra,C., Belin,C., Robert,N., Leung,J., Rodriguez,P.L., Lauriere,C. and Merlot,S. (2009). Protein phosphatases 2C regulate the activation of the Snf1-related kinase OST1 by abscisic acid in Arabidopsis. Plant Cell 21, 3170-3184.
Pubmed: Author and Title
CrossRef: Author and Title
Google Scholar: Author Only Title Only Author and Title

Wang, F., Zhu, D., Huang, X., Li, S., Gong, Y., Yao, Q., Fu, X., Fan, L.M., and Deng, X.W. (2009). Biochemical insights on degradation of Arabidopsis DELLA proteins gained from a cell-free assay system. Plant Cell 21, 2378-2390.
Pubmed: Author and Title
CrossRef: Author and Title
Google Scholar: Author Only Title Only Author and Title

Wang, P., Xue, L., Batelli, G., Lee, S., Hou, Y.J., Van Oosten, M.J., Zhang, H., Tao, W.A., and Zhu, J.K. (2013). Quantitative phosphoproteomics identifies SnRK2 protein kinase substrates and reveals the effectors of abscisic acid action. Proc. Natl. Acad. Sci. USA 110, 11205-11210.
Pubmed: Author and Title
CrossRef: Author and Title
Google Scholar: Author Only Title Only Author and Title

Yin, X.J., Volk, S., Ljung, K., Mehlmer, N., Dolezal, K., Ditengou, F., Hanano, S., Davis, S.J., Schmelzer, E., Sandberg, G., Teige, M., Palme, K., Pickart, C., and Bachmair, A. (2007). Ubiquitin lysine 63 chain forming ligases regulate apical dominance in Arabidopsis. Plant Cell 19, 1898-1911.
Pubmed: Author and Title
CrossRef: Author and Title
Google Scholar: Author Only Title Only Author and Title

Yoshida, T., Nishimura, N., Kitahata, N., Kuromori, T., Ito, T., Asami, T., Shinozaki, K., and Hirayama, T. (2006). ABA-hypersensitive germination3 encodes a protein phosphatase 2C (AtPP2CA) that strongly regulates abscisic acid signaling during germination among Arabidopsis protein phosphatase 2Cs. Plant Physiol. 140, 115-126.
Pubmed: Author and Title
CrossRef: Author and Title
Google Scholar: Author Only Title Only Author and Title

Yu,F., Wu,Y. and Xie,Q. (2016). Ubiquitin-Proteasome System in ABA Signaling: From Perception to Action. Mol. Plant 9, 21-33.
Pubmed: Author and Title
CrossRef: Author and Title
Google Scholar: Author Only Title Only Author and Title

Zhang, X., Garreton, V., and Chua, N.H. (2005). The AIP2 E3 ligase acts as a novel negative regulator of ABA signaling by promoting ABI3 degradation. Genes Dev. 19, 1532-1543.
Pubmed: Author and Title
CrossRef: Author and Title
Google Scholar: Author Only Title Only Author and Title

Zhang, X., Wu, Q., Ren, J., Qian, W., He, S., Huang, K., Yu, X., Gao, Y., Huang, P., and An, C. (2012). Two novel RING-type ubiquitin ligases, RGLG3 and RGLG4, are essential for jasmonate-mediated responses in Arabidopsis. Plant Physiol. 160, 808-822.
Pubmed: Author and Title
CrossRef: Author and Title
Google Scholar: Author Only Title Only Author and Title

Zhang, X., Wu, Q., Cui, S., Ren, J., Qian, W., Yang, Y., He, S., Chu, J., Sun, X., Yan, C., Yu, X., and An, C. (2015). Hijacking of the jasmonate pathway by the mycotoxin fumonisin B1 (FB1) to initiate programmed cell death in Arabidopsis is modulated by RGLG3 and RGLG4. J. Exp. Bot.66, 2709-21

Pubmed: Author and Title
CrossRef: Author and Title
Google Scholar: Author Only Title Only Author and Title

Zhao,Y., Xing,L., Wang,X., Hou,Y.J., Gao,J., Wang,P., Duan,C.G., Zhu,X. and Zhu,J.K. (2014). The ABA receptor PYL8 promotes lateral root growth by enhancing MYB77-dependent transcription of auxin-responsive genes. Sci. Signal. 7, ra53.

Pubmed: Author and Title
CrossRef: Author and Title
Google Scholar: Author Only Title Only Author and Title

Zhao,J., Zhou,H., Zhang,M., Gao,Y., Li,L., Gao,Y., Li,M., Yang,Y., Guo,Y. and Li,X. (2016). Ubiquitin-specific protease 24 negatively regulates abscisic acid signalling in Arabidopsis thaliana. Plant Cell Environ. 39, 427-440.

Pubmed: Author and Title
CrossRef: Author and Title
Google Scholar: Author Only Title Only Author and Title

Zhu, S.Y., Yu, X.C., Wang, X.J., Zhao, R., Li, Y., Fan, R.C., Shang, Y., Du, S.Y., Wang, X.F., Wu, F.Q., Xu, Y.H., Zhang, X.Y., and Zhang, D.P. (2007). Two calcium-dependent protein kinases, CPK4 and CPK11, regulate abscisic acid signal transduction in Arabidopsis. Plant Cell 19, 3019-3036.

Pubmed: Author and Title
CrossRef: Author and Title
Google Scholar: Author Only Title Only Author and Title